COASTAL BIOGEOCHEMICAL AND MICROBIAL RESPONSES TO EXPORTS FROM A SMALL RAIN-DOMINATED RIVER PLUME IN THE NORTHEAST PACIFIC COASTAL TEMPERATE RAINFOREST

Student: REBECCA WHALEN

Supervisor: DR. KYRA ST. PIERRE

Thesis submitted to the University of Ottawa in partial Fulfillment of the requirements for the M. Sc. Degree in Earth Sciences

uOttawa

Department of Earth and Environmental Science, Faculty of Science

Table of Contents

Chapter 1: Thesis Introduction

Thesis Abstract

The Northeast Pacific Coastal Temperate Rainforest (NPCTR) spans over 2000 km from Alaska to California and includes 1000's of diverse small rain-dominated coastal watersheds that, despite covering 24% of the surface area, deliver 33% of discharge to the Pacific Ocean. Coastal ecosystems receiving these inputs are potential hotspots of biogeochemical transformation but remain understudied due to logistical and historical biases of the fields of oceanography and limnology. This lack of integration across these fields limits our understanding of how terrestrial exports from small catchments affect coastal carbon and nutrient dynamics, microbial community structure, and overall ecosystem ecology.

This thesis addresses this problem by examining a river-ocean estuary on Quadra Island (British Columbia, Canada) to assess how rain-dominated watershed exports shape coastal microbiology and biogeochemistry. Water samples collected within a small river plume (0-27.9 PSU) at 0, 15, and 50 cm depth across seven sites from Hyacinthe Creek into Hyacinthe Bay were analyzed for phosphate, silica, carbon and nitrogen species and isotopes, dissolved organic matter (DOM) composition, and putative active (RNA) and present (DNA) microbial communities. The core of this thesis is a manuscript that analyses carbon and nutrient concentrations, stable isotope signatures, and microbial community diversity to investigate how vertical and horizontal salinity gradients affect dispersion of organic and inorganic matter, and its potential effects on microbial ecology.

Surface samples and salinity mapping revealed distinct biogeochemical and microbial signatures relative to underlying waters, dissipating with increasing distance from the creek mouth. Nutrient and organic matter concentrations and signatures increased with distance from the creek mouth, deviating from conservative mixing and suggesting active reprocessing. Microbial communities exhibited distinct horizontal and vertical structures, supporting the existence of a river-to-sea microbial continuum, and revealing taxa that may be disproportionately more active compared to the total community in transitional waters. Salinity, organic carbon, condensed aromatic compounds, and isotopic signatures (δ^{13}C-DOC, δ^{13}C-POC, δ^{15}N-PN) were highlighted as key drivers of coastal microbial community structure. Cumulatively, this study explores important biogeochemical trends through small-scale vertical and horizontal extents, a scale often overlooked in oceanography and larger river plume systems. This work further highlights that small, rain-dominated river plumes may strongly influence biogeochemical cycling and microbial dynamics in NPCTR estuaries, and that their impacts are concentrated in a vertically shallow but active surface layer. This estuary approach advances our current understanding of biogeochemical dynamics in small rain-dominated river plumes of the NPCTR, while suggesting the need for a finer-resolution lens to study small rain-dominated watersheds in future.

Thesis Acknowledgements

This thesis would not have been possible without the community that supported me throughout the process. From classmates, friends, and family to my lab group, co-authors, and supervisor, all have been instrumental in this research.

Firstly, I would like to acknowledge Dr. Kyra St. Pierre for your willingness to take a chance on a student you had never met, first as an Honour's student and later as an accelerated Master's student. Your consistent passion and encouragement gave me the space to see my full potential on this project. I believe I speak not only for myself, but also for the many students you have supervised and will continue to supervise, in saying that I could not have asked for a better mentor. You have created an atmosphere within the L2O Biogeochemistry Lab that has been a highlight of both of my degrees. From bi-weekly meetings discussing ethical and impactful research to advising on figures and content, this thesis is as much mine as the many individuals who helped shape this work. Isabel, Kate, Jess, Chantal, Alessandra, Brogan, Leif, Paisley, Trishna, Jaida, Zac, and Christine, thank you for your guidance, collaboration, and unwavering support.

Along the way, I have received guidance from not only my supervisor, but many incredible scientists. To my co-authors, your input and guidance have been deeply influential. Without the resources and knowledge you have shared with me, this project may have never become what it is. Furthermore, this project would not have been possible without the contributions of the following institutions: the Hakai Institute with the Tula Foundation, the University of British Columbia, the University of Ottawa, the University of Alberta, Toronto Metropolitan University, and the Pacific Salmon Foundation, whose resources, infrastructure, and research contributions made this work possible. Thank you to the laboratories that analysed this study's samples: the Ján Veizer Stable Isotope Laboratory, UC Davis Stable Isotope Laboratory, the University of British Columbia's Marine Zooplankton and Micronekton Laboratory and the University of Alberta Biogeochemical Analytical Service Laboratory. I also extend my appreciation to Natalie Benoit from the University of British Columbia and Emily Haughton from the Hakai Institute for their guidance and support throughout this project.

To my undergraduate and graduate professors, namely Brett Walker, who initially referred me to Kyra, Oliver Warr, who has always shown enthusiasm for everything I do, and Bahram Daneshfar, who shared their insight into my ArcGIS work, you have all contributed meaningfully to this thesis.

Lastly, I genuinely would not have been able to accomplish all that I have without my family and friends. To Mom, Dad, Nana, Grampie, Nena, Jordyn, Grayson, Breanna, Lucas, Tom, Benita, Alyssa, Libby, Makenna, Doga, Hannah, James, you all inspire me every day to be the best version of myself. Your encouragement has shaped both the person I have become and the path that brought me here. Your support, in all its forms, means more to me than I can express.

List of Figures

List of Tables

Glossary

POC = Particulate organic carbon

DOC = Dissolved organic carbon

TOC = Total organic carbon

DOM = Dissolved organic matter

OM = Organic matter

NOM = Natural Organic Matter

NH_4^+ = Ammonia

NO_3^- = Nitrate

TN = Total nitrogen

DN = Dissolved nitrogen

PN = Particulate nitrogen

DON = Dissolved organic nitrogen

DIN = Dissolved inorganic nitrogen

PO_4^{3-} = Phosphate

SiO_2 = Silica

RDA = Redundancy Analysis

PCA = Principal Component Analysis

ANOVA = Analysis of Variance

LMM = Linear Mixed Model

NPCTR = Northeast Pacific Coastal Temperate Rainforest

CTR = Coastal Temperate Rainforest

RHC = Rain Hills-Central (Watershed Classification)

FT-ICR-MS = Fourier Transform Ion Cyclotron Resonance Mass Spectrometry

MAAT = Mean Annual Air Temperature

MAP = Mean Annual Precipitation

Statement of Authorship Contributions

Data compilation and analysis, figure generation, and writing were conducted by Rebecca Whalen (RW), under the guidance and supervision of Kyra St. Pierre (KSP), with additional input from co-authors. Chapters 1 and 3 were written by RW, with comments and feedback from KSP. Chapter 2, prepared as a manuscript for submission to Estuaries and Coasts, was drafted, incorporating feedback from KSP, Colleen Kellogg (CK; Hakai Institute), and Ian Giesbrecht (IG; Hakai Institute). Suzanne Tank (ST; University of Alberta), Lauren Portner (LP; Pacific Salmon Foundation), Isabelle Desmarais (ID: Hakai Institute), Ryan Hutchins (RH; Toronto Metropolitan University), and Brian Hunt (BH; UBC) also provided feedback on the results and were involved in the study design, fieldwork and/or laboratory analyses. Initial study design was conducted by KSP with BH, ST, and IG. Fieldwork was led by KSP, with CK, LP, and ID. Samples analyses were performed at the Hakai Institute, University of Ottawa's Ján Veizer Stable Isotope Laboratory, University of California Davis Stable Isotope Laboratory, and the University of Alberta Biogeochemical Analytical Service Laboratory. CK and RH processed amplicon sequencing and FT-ICR-MS data, respectively, and provided supporting information to RW. CK wrote the methodology section for *Microbial Community Profiling Using Amplicon Sequencing*. We declare no conflicts of interest relevant to this study. We declare no ethics approval was required. The research funding was supported by the Tula Foundation and the University of British Columbia.

Background and Literature Review

Coastal river plumes as critical integrators of terrestrial and marine forces

Coastal ocean waters have emerged as critical ecosystems at the interface of the land, ocean, and atmosphere (Bianchi et al., 2014). These regions provide essential ecosystem services, including carbon sequestration, raw material extraction, aquaculture and fisheries, biodiversity support, coastal protection, water regulation, nutrient cycling, recreation and tourism, collectively accounting for 77% of global ecosystem-services values (Costanza et al., 1998; Kim et al., 2021; Martínez et al., 2007; Yao et al., 2024). Rivers and creeks account for over a third of land-based precipitation delivered to these coastal zones (Horner-Devine et al., 2015), providing a major pathway for elements that drive biological productivity, such as carbon, nitrogen, phosphorus, iron and silica, to enter the global oceans (Bianchi et al., 2014).

The most ubiquitous interactions between freshwater and marine systems occur as the river discharges into the coastal ocean, commonly referred to as a *river plume*. River plumes are a region of freshwater influence characterized by a buoyant, low-salinity surface layer overlying salinity-rich marine waters (Bianchi et al., 2014; F. Chen & MacDonald, 2006; Horner-Devine et al., 2015; O'Donnell et al., 2008). The size and structure of river plumes vary widely, and are controlled by processes such as freshwater discharge, dilution rates, vertical mixing, and transport by horizontal advection (Horner-Devine et al., 2015). Given the vital role of the coastal oceans in climate change mitigation, improving our understanding river-ocean dynamics is increasingly important within the fields of oceanography and limnology.

Our current understanding of freshwater-ocean connections is primarily derived from work conducted on large river plumes/drainage systems (> 9 000 km^2) and fjords, which are relatively larger, deeper, isolated systems of high local importance, experiencing rapid responses to climate change impacts (Bertin et al., 2025; Bianchi et al., 2020; Dagg et al., 2004; Horner-Devine et al., 2015; Hunt et al., 2024; Vargas et al., 2011). Smaller plumes experience freshwater inputs at smaller discharge rates (0.1 – 30 $m^3 s^{-1}$), producing a quickly decelerating inertial jet, spreading based on buoyancy and tides (Basdurak et al., 2020; Hunt et al., 2024). In comparison to large plumes, small river plumes' freshwater discharge is estimate to be limited to the surface waters (thickness of a few tens of cm) and dissipate within 0.1 to 3 km of the discharge location (Basdurak et al., 2020; Hunt et al., 2024).

The cumulative effect of multiple sources of freshwater discharge to the coastal ocean has led to the creation of localized trends in ocean circulation along the coasts in the Northern Hemisphere (Carmack et al., 2015; Hunt et al., 2024). The contiguous panarctic Riverine Coastal Domain (RCD) is study-specific example of freshwater driven impacts on ocean circulation, where riverine discharge and runoff of terrigenous materials have created a low-saline buoyancy-forced boundary that originates from the large freshwater exports from the Northeast Pacific Coastal Temperate Rainforest (NPCTR) and

extends clockwise around the entirety of North America (Carmack et al., 2015; Hunt et al., 2024). The narrow, shallow RCD affects offshore primary production, ocean acidification, light availability, nutrient and carbon regimes, and the dispersal and migration of marine biota (Carmack et al., 2015; Hunt et al., 2024).

Considering freshwaters function as vectors of nutrients and organic matter to coastal oceans (Anderson et al., 2020; Raymond et al., 2013; St. Pierre et al., 2020), framing land-to-ocean connections through an estuary meta-ecosystem lens can be key for addressing scientific knowledge gaps and cross-realm connectivity. A meta-ecosystem approach involves analyzing a series of regional ecosystems connected through the flow of materials and energy (Loreau et al., 2003; Menge et al., 2019), like the flow of biogeochemical constituents through a river plume (Bianchi et al., 2014). This perspective is a novel approach to understanding processes at the interfaces of local ecosystems and thus is key for exploring how spatial and vertical salinity gradients affect biogeochemical properties in coastal and estuarine zones (Loreau et al., 2003).

The Northeast Pacific Coastal Temperate Rainforest (NPCTR) as an important land-ocean interface

The NPCTR is the largest of all Coastal Temperate Rainforests (CTR) regions, globally (DellaSala, 2011; Hunt et al., 2024), extending over 2000 km along the coast of North America, from Alsek River, Alaska to Eel River, California (Bidlack et al., 2021; Hunt et al., 2024). This region spans a variety of climates from subpolar to temperate conditions with seasonal variation, perhumid conditions, and over 4000 mm of precipitation annually, the most of all eco-regions in North America (Bidlack et al., 2021; Hunt et al., 2024). Given its large geographic range, its coastlines are characterized by fjords, channels, bays, and islands (Hunt et al., 2024), with increasing snow and ice northwards, and glacier mass loss at one of the highest rates globally (Gardner et al., 2013; Hunt et al., 2024). NPCTR watersheds exhibit high diversity, with 14 categorical "types" defined by distinct combinations of climate, topography, and dominant freshwater sources (rain, snowmelt, glacial) (Figure 1), which in turn predict factors such as streamflow and carbon dynamics (Giesbrecht et al., 2022, 2025). The NPCTR's small rain-dominated watersheds are characterized by perhumid conditions and deep, organic-rich soils, that drive high DOC exports, an estimated 3.5 Tg-C yr^{-1} (McNicol et al., 2019; 2023), with mean annual discharge rates of 33% to the global ocean, despite accounting for 24.4% of the surface area (Giesbrecht et al., 2022, 2025). This region is critically important for Pacific Salmon, a keystone species, whose anadromous life cycle relies on the flow of nutrients and water between marine and freshwater ecosystems, reinforcing the reciprocal connection between land and ocean (Walsh et al., 2020). As such, small rain-dominated NPCTR watersheds are ideal for conducting land to ocean studies, as their coastal waters are potential hotspots for biogeochemical activity but remain understudied due to current limitations of limnology and oceanography (Bidlack et al., 2021).

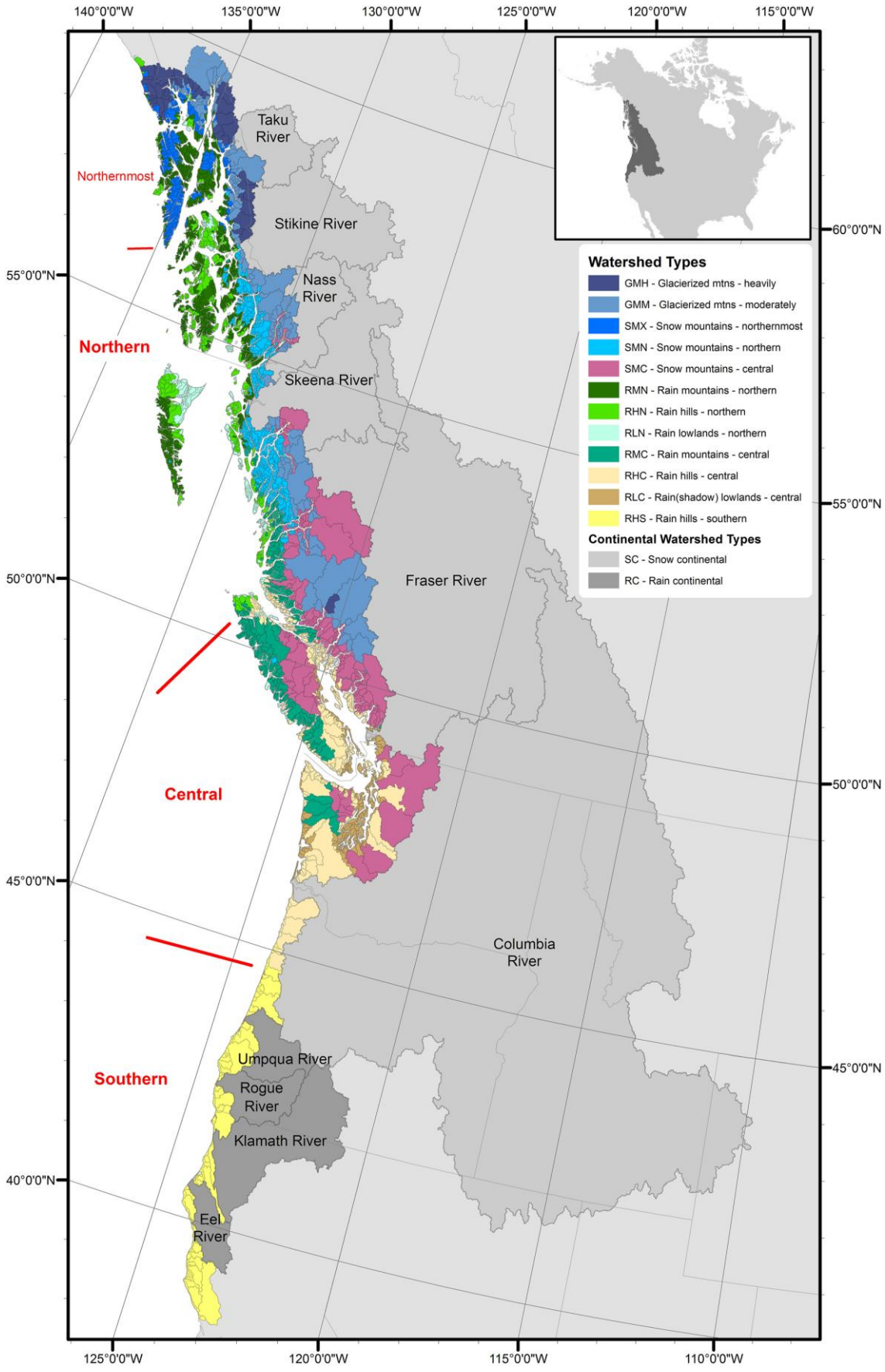

Figure 1: Map of 14 watershed classifications within the NPCTR margin, retrieved from (Giesbrecht et al., 2022).

Within the NPCTR, the study region is part of the *Rain hills – central (RHC)* watershed type, one of seven rain-dominated NPCTR watershed types (Figure 1 (Giesbrecht et al., 2022, 2025)). RHC watersheds account for 6.6% of the total surface area of the NPCTR while contributing to 4.5% of the mean annual discharge (MAD) (Giesbrecht et al., 2022, 2025). This watershed type is characterized by low to moderate relief, productive but disturbed forests, deep mineral flow paths, and a climate affected by the rain shadow created by coastal mountain ranges (Giesbrecht et al., 2025). In terms of water quality, the waters are clear to humic stained in colour, with moderate dissolved organic matter (DOM) and pH, and high inorganic nutrients, weathering solutes, and buffering capacity (Giesbrecht et al., 2025). While RHC consists of 626 small watersheds (mean area = 4 km^2), their combined input makes it the second-largest contributor among rain-dominated watersheds in the NPCTR (Giesbrecht et al., 2022, 2025).

Nutrient and organic matter dynamics in coastal plumes

This study examines the biogeochemical cycling of macronutrients and organic matter, specifically nitrogen (N), phosphorous (P), silicon (Si), and carbon (C) within a small river plume of the NPCTR. These elements are fundamental components of biomolecules and important drivers in regulating biological production in coastal plume systems, where they are taken up, transformed, and recycled by microbial communities (da Cunha, 2020; McNicol et al., 2023).

In aquatic environments, nutrients and organic matter originate from multiple sources, experiencing varied transformation pathways. Allochthonous inputs derive from terrestrial materials such as plant litter and soil organic matter, whereas autochthonous sources are produced within the aquatic ecosystem through phytoplankton growth and microbial production (Sleighter & Hatcher, 2008). Thus, small river plumes are particularly important, as they serve as a vector for both natural and anthropogenically derived nutrients and organic matter from land to the coastal ocean (St. Pierre et al., 2021). Although rivers represent a major pathway for the ocean-ward transport of materials, they are not the sole contributors. Atmospheric deposition, sediment resuspension, and groundwater discharge can supply copious quantities of nutrients and organic matter to coastal oceans (Howarth & Marino, 2006). However, this study focuses solely on the riverine contributions to coasts.

In aquatic ecosystems, nitrogen is found in a wide range of inorganic (nitrate (NO_3^-), nitrite (NO_2^-), ammonium (NH_4^+), ammonia (NH_3), nitrous oxides (NO_x), and nitrogen gas (N_2)), and organic (e.g., urea, amino acids; collectively dissolved organic nitrogen (DON)) species in both dissolved and particulate (PN) pools, making it one of the most chemically and microbially complex nutrient cycles (Howarth & Marino, 2006). Its cycling is mediated by a suite of microbially driven redox transformations, including mineralization (OM → NH_3/NH_4^+ → NO_2^-/NO_3^-) and ammonification (OM → NH_4^+/ NH_3 or NO_2^- → NH_3/NH_4^+) of organic matter (OM), nitrification (NH_3/NH_4^+ → NO_2^-/NO_3^-), denitrification (NO_2^- → N_2O → N_2), anammox (NH_4^+/NO_2^- → N_2), assimilation (NH_3/NH_4^+ → OM), nitrogen fixation (N_2 → NH_3/NH_4^+), and both assimilatory and

dissimilatory nitrate reduction ($NO_3^- \rightarrow NO_2^- \rightarrow NH_3/NH_4^+$ & $NO_3^- \rightarrow NO_2^-$) (Herbert, 1999). These processes are conducted by a diverse array of autotrophic and heterotrophic microbes in response to redox gradients, and availability of oxygen and carbon sources (Herbert, 1999; Howarth & Marino, 2006). This sensitivity suggests that physical characteristics of the environment, such as stratification, mixing, and freshwater discharge will likely regulate nitrogen cycling and transformations in river plumes, with further consequences on availability and productivity downstream (Haas et al., 2021; Voss et al., 2013).

In contrast to nitrogen, bioavailable phosphorus in aquatic systems is simply dominated by orthophosphate, hereafter referred to as phosphate (PO_4^{3-}), with some contributions from dissolved and particulate organic phosphorous, which must be remineralized to PO_4^{3-} before use by primary producers (Benitez-Nelson, 2000; Correll, 1999; Howarth & Marino, 2006). Low freshwater exports of PO_4^{3-} are common due to the strong sorption of PO_4^{3-} with minerals and organic particles through retention and sediment burial (Benitez-Nelson, 2000; Correll, 1999). To have bioavailable PO_4^{3-}, it must then be mobilized via mineral weathering, erosion, and desorption (i.e., leaching) from those sediments (Howarth & Marino, 2006).

Inorganic forms of nitrogen (NO_3^-, NH_4^+) and PO_4^{3-} can be important limiting nutrients to primary producers and coastal productivity, but their limitations differ depending on the aquatic ecosystem type (Howarth & Marino, 2006). A limiting nutrient is that which limits primary producer growth based on its quantity relative to other nutrients required (Correll, 1999; Harris, 1986; Howarth & Marino, 2006). In low supply, it limits the growth of primary producers and coastal productivity, whereas in excess, it leads to excessive growth of algal populations, increasing the potential for harmful algal blooms, and contributing to coastal eutrophication, and global dead zones (Gobler, 2020; Howard et al., 2022; Howarth & Marino, 2006; Ngatia et al., 2019). It is widely accepted that nitrogen is limiting in marine environments, and phosphorous is limiting in freshwaters (Howarth & Marino, 2006). This is due, in part, to desorption of phosphorous bound to sediments and increased remineralization of organic phosphorous with changes in redox, pH, and increased salinity making it increasingly more available than in freshwaters (Maranger et al., 2018; Ngatia et al., 2019). Conversely, nitrogen fixation by plankton is reduced in highly saline environments (Ngatia et al., 2019). The molar ratio of dissolved inorganic nitrogen (sum of NO_3^- and NH_4^+) to total phosphorous (DIN:TP) is currently the most commonly used indicator of potential nutrient limitation in aquatic systems (Howarth & Marino, 2006), through comparison with the Redfield ratio (106:16:1 = C:N:P), a consistent molar ratio of carbon to nitrogen to phosphorous found in marine phytoplankton (Redfield, 1960).

The dominant form of silicon (Si) in aquatic ecosystems is silicic acid ($Si(OH)_4$), a hydrated version of silica (hereafter SiO_2), produced via chemical weathering of soil and geologically derived silicates (Bernard et al., 2011). Estuarine environments and coastal river plumes are primary vectors of SiO_2 from land to ocean, characterized by increased mixing, diatom uptake, and dissolution of riverine SiO_2 (Bernard et al., 2011; Yool & Tyrrell, 2003). Diatoms are an important group of primary producers, accounting for 40% of the marine productivity, with a special interest in SiO_2 for building their distinctive

opaline silica frustules (Q. Chen et al., 2025; Yool & Tyrrell, 2003). Temperate regions often observe large diatom blooms when SiO_2 is abundant, followed by sharp declines in diatom biomass and shifts in community composition once it becomes limiting, typically during the spring (Krause et al., 2018).

Aquatic carbon is found as dissolved inorganic carbon (DIC; sum of CO_2, H_2CO_3, HCO_3^-, and CO_3^{2-}) and dissolved and particulate organic carbon (DOC/POC: sugars and organic acids derived from living organisms) (Maranger et al., 2018; McNicol et al., 2023). DIC is the main carbon reservoir, contributing to global warming through greenhouse gas emissions, while also supporting autotrophic production by aquatic microbial species (Raymond et al., 2013). DOC and POC are carbon species that can be respired, transformed, transported or buried, and can be taken up by heterotrophic microbial species (Anderson et al., 2020). While distinct, the varying forms of carbon are intrinsically linked to coastal zones as they form the basis for photosynthesis and respiration, with further impacts on microbial diversity (Anderson et al., 2020; Jiao et al., 2014). DOC is often the dominant carbon species that is exported to coastal oceans through the freshwater pipe, specifically in the study region (McNicol et al., 2023). In these coastal zones, carbon species concentrations are strongly constrained by riverine discharge and upwelling, with their dynamics driven by primary productivity, remineralization, and particle aggregation, making plumes a potential hotspot of carbon cycling and gas exchange (Bidlack et al., 2021; McNicol et al., 2023).

Carbon and nitrogen stable isotope signatures can be useful parameters for measuring sources of organic matter and nutrients across transitional environments, given that signatures are typically distinct between allochthonous and autochthonous sources, and freshwaters typically possess a unique isotopic signature compared to seawater and estuaries (Murphy et al., 2008; Yu et al., 2010). Carbon has two stable isotopes: ^{13}C and ^{12}C, with abundances of 1.1% and 98.8% respectively, the ratio of which can provide valuable insight into its sources (Mook, 2000). The general range of δ^{13}C-DOC and POC (‰) in freshwater is between -30 and -25‰, whereas marine plankton is closer to -20‰ (Mook, 2000). Nitrogen has two naturally occurring stable isotopes: ^{15}N and ^{14}N with abundances of 0.37% and 99.63%, respectively (Mook, 2000). This study looks at three isotopic compositions (in per mil, ‰): δ^{13}C-DOC, δ^{13}C-POC, δ^{15}N-PN, calculated as follows:

[Eq. 1] $$\delta^{13}\mathrm{C}\ ‰ = \left(\frac{\left(\frac{\delta^{13}\mathrm{C}}{\delta^{12}\mathrm{C}}\right)_{sample}}{\left(\frac{\delta^{13}\mathrm{C}}{\delta^{12}\mathrm{C}}\right)_{standard}} - 1\right) \times 100$$ and [Eq. 2] $$\delta^{15}\mathrm{N}\ ‰ = \left(\frac{\left(\frac{\delta^{15}\mathrm{N}}{\delta^{14}\mathrm{N}}\right)_{sample}}{\left(\frac{\delta^{15}\mathrm{N}}{\delta^{14}\mathrm{N}}\right)_{standard}} - 1\right) \times 100.$$

Freshwater-seawater conservative mixing plots are a method for evaluating chemical concentrations and isotopic signatures by creating a simple two end-member mixing model based on freshwater and marine end-members (Eq. A1, Eq. A2, Fry, 2002). Deviations from these mixing models can provide insight into within-estuary organic matter reprocessing (Fry, 2002), highlighting regions along the salinity continuum where processes other than simple physical water column mixing are adding or removing material (Loder & Reichard, 1981; Plont et al., 2023). Scatter points which fall above the mixing line imply in-

estuary sources or production (i.e., remineralization, desorption, in situ primary production), whereas points below the mixing line imply sinks or losses (i.e., biological uptake, flocculation, sorption to particles, degassing, or preferential removal of isotopically heavy fractions) (Fry, 2002; Loder & Reichard, 1981; Plont et al., 2023).

Dissolved organic matter (DOM) is a highly diverse pool of carbon-containing molecules, of which DOC is a component (Hutchins et al., 2017; Medeiros et al., 2016; Sipler et al., 2017; Vähätalo et al., 2011; Wang et al., 2021). Composed of a complex mixture of biomolecules (e.g., amino acids, carbohydrates, lipids, and lignin-derived aromatics), DOM results from the transformation of plant, animal, and microbial matter, and accounts for the dissolved fraction of natural organic matter (NOM) (Qi et al., 2022; Sleighter & Hatcher, 2008). DOM is transformed through microbial or photochemical processes, where solar radiation breaks down complex organic molecules into simpler forms for microbial assimilation (St. Pierre et al., 2021). It is a crucial contribution to the global carbon and nutrient cycles, as it can be building blocks and energy sources for aquatic communities when converted into inorganic carbon, while equally contributing to carbon sequestration in aquatic ecosystems (Qi et al., 2022; Sleighter & Hatcher, 2008; Vargas et al., 2011).

A commonly used technique for characterizing and analyzing DOM is through Fourier Transform Ion Cyclotron Resonance Mass Spectrometry (FT-ICR-MS) (Qi et al., 2022). Though FT-ICR-MS possesses the highest mass solving power (R = 3 000 000) and best mass accuracy (MA = m/z from 260-1500), it is still widely considered to be a primarily qualitative analysis of DOM composition, based on verified peak analysis and ratios (Qi et al., 2022). The resulting dataset contains the following raw variables: m/z (mass-to-charge ratio of the detected ion), H, O, C, N, S, P (number of elemental atoms in the assigned formula), H/C (hydrogen to carbon ratio, indicating saturation level, where higher H/C is more aliphatic (i.e., saturated)), and O/C (oxygen to carbon ratio, indicate oxidation state, where higher O/C suggests higher polarity and biodegradability) (Qi et al., 2022). Given these raw variables, indices can be derived that allow one to classify the samples by compound classes; the main derived indices are double bond equivalents (DBE), a measure of unsaturation (i.e., double bonds), and the modified aromaticity index (AI_{mod}), a calculated index to assess aromaticity (Eq. 9, Appendix C) (Qi et al., 2022).

The resulting FT-ICR-MS derived indices and raw variables (H/C, O/C, DBE, AI_{mod}) can thus create meaningful categorical classifications about the composition of DOM in samples (Qi et al., 2022). It does so by classifying based on five compound classes (Table 1): aliphatics, aromatics/polyphenols, condensed aromatics, high-oxygen (high-O) and low-oxygen (low-O) unsaturated compounds, revealing the samples' role in biogeochemical processes (e.g. origin, storage, transport, decomposition, and release of greenhouse gases) (Qi et al., 2022). Studies suggest that freshwater or terrestrial derived OM may be more aromatic and oxygen rich whereas marine OM is more aliphatic and oxygen poor (Sleighter & Hatcher, 2008). Other meaningful analysis can manifest as CHON percent relative abundance analysis and C/N ratios to determine nitrogen elemental variation along the salinity gradient(s). Studies show that CHON compounds are negatively correlated with salinity (Chen et

al., 2023), becoming more structurally diverse throughout the plume with increased N, S, and P-containing compounds (Sleighter & Hatcher, 2008).

DOM is of particular importance to microbial species, as they can use DOM as a carbon or nutrient source, supporting cellular respiration and photosynthesis. Incubation of complex DOM mixtures with microbial species resulted in changes in characterization over time; initially the sediment-derived DOM was enriched in protein-like compounds (i.e., CHON) and highly labile carbon (i.e., aliphatic compounds), which was rapidly utilized by species such as *Pseudomonas, Burkholderiales, Chitinophagales*, and *Rhodobacterales,* and disappeared within 1.5 days (Wu et al., 2018). This resulted in a metabolic shift from activity and growth to maintenance, where the intensity of genes involved in transforming labile C decreased and plateaued, and the genes involved in recalcitrant C and phenol oxidases (i.e., aromatics) increased significantly, supporting species such as *Xanthomonadales, Sphingomonadales, Rhodospirillales, Rhizobiales*, and *Nitrosomonadales* (Wu et al., 2018).

Table 1: Classification criteria for FT-ICR-MS derived compound classes (aliphatics, aromatics, condensed aromatics, low-O unsaturated, and high-O unsaturated compounds). Information retrieved from (Koch & Dittmar, 2006; Orlova et al., 2024; Qi et al., 2022; Ren et al., 2024).

Compound type	Classification criteria	Meaning
Aliphatic	$H/C > 1.5$	Saturated compounds (i.e., lipids, proteins, and carbohydrates)
Condensed Aromatics	$AI_{mod} \geq 0.67$	Recalcitrant, combustion-derived materials (i.e., black carbon)
Aromatic/Polyphenol	$0.5 < AI_{mod} < 0.67$	Multiple phenol groups
Low-O Unsaturated	$H/C < 1.5$, $AI_{mod} < 0.5$, $O/C < 0.5$	Less unsaturated hydrocarbons or less oxidized aromatics
High-O Unsaturated	$H/C < 1.5$, $AI_{mod} < 0.5$, $O/C \geq 0.5$	More polar or oxidized structures

Within the NPCTR, terrestrial exports of nutrients and organic matter vary with respect to watershed geomorphology, freshwater discharge volume, and timing of seasonal events and transitions (Hunt et al., 2024). While freshwater systems see increased organic matter and nutrient exports during the wet season (December to February), marine productivity typically follows an inverse pattern, with early spring phytoplankton blooms as light availability increases and freshwater inputs decline (Hunt et al., 2024). The NPCTR and similar CTR regions globally exhibit generalized terrestrial macronutrient concentration ranges of < 2 μM to > 10 μM [NO_3^-], < 0.1 μM [PO_4^{3-}], and > 40 μM [$Si(OH)_4$] (Hunt et al., 2024). Work conducted on rain-dominated watersheds (*Rain-Hills North* type; Giesbrecht et al. 2022) of the Central Coast of British Columbia, within the heart of the NPCTR, indicates that freshwater exports from small river plumes dilute coastal inorganic nutrient concentrations in the region (e.g., nitrate and phosphate), while enhancing organic-matter-associated nutrient concentrations (e.g., DOC, DON) (Hunt et al., 2024; St. Pierre et al., 2021). While yields of DOC and DON for the region are estimated to be among the largest globally (St. Pierre et al. 2021), much of the integrative work assessing coastal water responses to small river contributions in the NPCTR has been focused on southeast Alaska and the Central Coast of British Columbia, where soil organic carbon stocks and therefore DOC concentrations are among the highest globally for coastal river systems (McNicol et al., 2023; Oliver et al.,

2017). Comparatively less is known about how coastal waters reprocess the exports from other watershed types in the region (Giesbrecht et al., 2022, 2025a; Hunt et al., 2024; McNicol et al., 2023). Further characterization of coastal biogeochemistry is needed to understand spatial variations in how terrestrial exports affect coastal biogeochemistry (Hunt et al., 2024; St. Pierre et al., 2020).

Microbial communities as drivers of nutrient and carbon cycling in coastal river plumes

Microbes are tiny living organisms that can only be seen under a microscope, including bacteria, viruses, fungi, protozoa, and photosynthetic organisms like cyanobacteria and phytoplankton (Sreeharsha & Venkata Mohan, 2024). Microbes are at the forefront of nutrient dynamics and biogeochemical cycling of carbon, nitrogen, phosphorous, sulfur, and silica in coastal ecosystems (Sipler et al., 2017). They mediate transformations of macronutrients and complex organic matter by converting dissolved, particulate, and elemental forms into simple, biologically available forms (Sleighter & Hatcher, 2008). Microbial species, in particular autotrophs, are key parts of aquatic food chains, often supporting higher trophic levels through these transformations, further linking terrestrial exports of organic and inorganic matter to marine ecosystems (Sipler et al., 2017). Variation in nutrient and OM supply and availability can impact metabolism of microbial taxa, further impacting their community composition and fundamental niches (Seelen et al., 2025; Sipler & Bronk, 2015). In this study, we distinguish between prokaryotes (bacteria and archaea) and photosynthetic microbial eukaryotes (phytoplankton), while recognizing and referring to the cumulative microbial community.

An important aspect of environmental microbiology is microbial metabolism, which is highly constrained by both the energy source and carbon source for transformations (Madsen, 2008). In terms of energy sources, there are two major pathways: photosynthetic organisms, which utilize energy from light (i.e., photons), and chemosynthetic organisms, which utilize energy from oxidizing reduced chemicals (litho-: inorganic reduced chemicals; organo-: organic reduced chemicals) (Table 2; Madsen, 2008). For carbon sources, autotrophs gain carbon from CO_2 fixation (i.e., they make their own food), whereas heterotrophs gain carbon from organic matter (Table 2; Madsen, 2008). Microbial species will find a functional niche that will supply them with their biological needs, but in some cases, species can change energy sources when their primary source is depleted (i.e., mixotrophs (Madsen, 2008)). Therefore, microbial metabolism and nutrient and organic matter availability are intrinsically linked as the main processes at the microscopic level are powered by various inorganic and organic matter in the water column (Madsen, 2008).

Table 2: Parameters constraining microbial identification based on metabolism (Madsen, 2008).

Energy source		**Chemical, organic**	**Chemical, inorganic**	**Light**
Carbon source	Fixed organic	Chemosynethic organoheterotroph	Chemosynthetic lithoheterotroph	Photosynthetic heterotroph
	CO_2(g)		Chemosynthetic lithoautotroph	Photosynthetic autotroph

Microbes thus regulate the pathways and transformations of nutrients and organic matter in coastal zones. They regulate inorganic and organic carbon through respiration, and DOM modification by photochemical and microbial processing of labile terrestrial derived DOM to semi-refractory marine DOM (Madsen, 2008; Shen & Benner, 2018; Sreeharsha & Venkata Mohan, 2024; Zhang et al., 2023). Microbes also drive nitrogen cycling in coastal waters, by mediating processes such as assimilation, nitrification, denitrification, anammox, and nitrogen fixation (Herbert, 1999; Zeglin, 2015). As for phosphorous cycling, microbes participate in remineralization of organic phosphorous and sorption of inorganic phosphorous, affecting bioavailability in coastal zones (Benitez-Nelson, 2000; Correll, 1999). Silica is specifically important to diatoms, and thus microbial-driven silicification is important for the availability of SiO_2 for frustule construction (Bernard et al., 2011; Yool & Tyrrell, 2003).

Coastal zones such as estuaries, brackish lakes, and bays often exhibit more diverse microbial processes and community composition compared to purely freshwater or marine ecosystems. Increased salinity can affect the solubility and availability of key organic matter and nutrients, leading to their precipitation or flocculation, affecting availability for biological uptake (Sipler & Bronk, 2015). In both sediment and aquatic environments, analysis of small sub-unit (SSU) ribosomal RNA (rRNA) and Braken2-estimated species abundance profiles has given rise to a phenomenon coined the *microbial river-to-sea continuum,* where increasing salinity leads to increased taxonomic differences, or decreased similarity in microbial species within the community (Tee et al., 2021). This difference is largely driven by horizontal and vertical salinity gradients and their corresponding variation in nutrient availability (Tee et al., 2021). These factors affect microbial community composition by altering fundamental niches and osmoregulation strategies, as many species are adapted to either saline or non-saline environments based on their physiological capacity to regulate internal salt balance (i.e., uptake and expulsion of salts such as Na^+ and K^+; Tee et al., 2021). Studies find that non-saline microbial species possess a high concentration of K^+ transporter genes, *kdp*, which are active in low external K^+ concentrations (i.e., freshwater ecosystems), whereas salinity adapted species have a more significant concentration of Na^+ transporter genes, *trkA,* essential under hyperosmotic stress (i.e., marine ecosystems) in order to export destabilized Na^+, and accumulate K^+ within cells (Tee et al., 2021).

Amplicon sequencing is a technique used in environmental microbiology and microbiome research for studying microbial diversity and community composition, by means of genomic sequencing directly from environmental samples (Baker et al., 2003; Hugerth & Andersson, 2017). Amplicon sequencing amplifies and sequences specific marker genes in 16S rRNA (in this study, the V4-V5 region), identifying microbial taxa by their unique sequence variations (Baker et al., 2003). This generates relative DNA and RNA counts from the total community, with DNA revealing who is present (i.e., standing stock) and RNA (converted to cDNA post-extraction) capturing the putatively active gene expression (i.e., rRNA from growing cells), highlighting active microbes from those that are dormant (Chícharo & Chícharo, 2008). The resulting combined DNA and

cDNA (i.e., RNA) libraries (ASVs) can be matched to microbial identities using a BLAST key, providing insight into qualitative measurements of putatively active microbes (by proxy of cDNA/RNA) and standing stock/abundance (by proxy of DNA). This method is useful as it is cost-effective and precise for taxonomy at the genus and family levels, but has primer limitations, leading to missing data around dinoflagellates, limiting full eukaryotic community profiling (Baker et al., 2003; Hugerth & Andersson, 2017).

Microbial ecology uses multivariate approaches as standard practice for linking environmental variables with amplicon sequencing results. Specifically, redundancy analysis (RDA) can be useful for assessing the influence of chemical, physical, or biological properties on community structure (Buttigieg & Ramette, 2014; Ramette, 2007). RDAs build on the same principle as principal component analysis (PCA), where the main axes, by means of multiple linear regressions are constrained by the environmental variables to explain the variance between independent and dependent variables (Buttigieg & Ramette, 2014; Ramette, 2007). With the use of two datasets, one for environmental variables (the independent variable), and species information (the dependent variable), RDAs create an ordination plot of microbial data with respect to the environmental variables (Buttigieg & Ramette, 2014; Ramette, 2007).

Knowledge gaps and study objectives

Despite recent work identifying NPCTR watersheds as areas of high dissolved organic carbon fluxes to the coastal ocean (Giesbrecht et al., 2022, 2025a; St. Pierre et al., 2020, 2021, 2022), small, shallow plumes, such as those in the RHC watersheds and their associated biogeochemical dynamics remain poorly characterized. Traditional oceanographic profiles typically only begin below 5 meters from the surface, completely missing this small freshwater plume, which likely only extends tens of centimeters deep in estuarine environments. This research gap is due, in part, to a lack of shared frameworks and methodology between traditional oceanography and limnology fields (Sahoo et al., 2025). Differences in terminology, data standards, scales, instrumentation, and the nature of the systems themselves make it challenging to transfer knowledge between these disciplines despite a common interest in aquatic ecosystems (Aoki et al., 2022; Sahoo et al., 2025).

The study area is defined as the *Hyacinthe Creek-Bay estuary* located along the central coastline of the NPCTR (Figure 2) in Quadra Island, British Columbia (approx. 50.13° N, 125.25° W). This region includes a freshwater watershed composed of five lakes, which flows through Hyacinthe Creek into the shallow marine bay of Hyacinthe Bay (Discovery Islands Forest Conservation Project, 2022). This watershed is home to a plethora of important flora and fauna, including Pacific salmon (Hunt

et al., 2024; Walsh et al., 2020). Given that the Hyacinthe Creek-Bay study site aligns with the characteristics defined as the Rain Hills-Central classification (RHC), it is a valuable model for similar watersheds within the NPCTR.

This study aims to address this knowledge gap by combining high-resolution vertical sampling of nutrient (nitrogen, phosphorus and silica), carbon, and organic matter dynamics, and microbial (prokaryote and eukaryote) communities along vertical and horizontal salinity gradients to characterize a small rain-dominated river plume along the coast of Quadra Island, in British Columbia, Canada (Hyacinthe Creek-Bay). The combined techniques from limnology and oceanography allows us to: (1) delineate the extent of the plume from a small rain-dominated system; (2) quantify and characterize nutrient concentrations, organic matter, and microbial community composition across the plume; to (3) link microbial community composition to carbon and nutrients at a resolution rarely addressed in the oceanography and limnology fields. This aims to address the research question; *How do riverine exports of nutrients and organic matter influence the putatively active microbes and biogeochemical cycling across small river plumes of the NPCTR?* We hypothesize that putatively active microbes, along with biogeochemical trends, will vary significantly across both horizontal and vertical salinity gradients in the Hyacinthe Creek–Bay estuary due to fundamental niche shifts caused by increased salinity and nutrient gradients, with the strongest signals expected in surface waters most directly influenced by freshwater inputs.

Chapter 2: Manuscript

Land-to-Ocean Biogeochemical Gradients Detected in a Small and Shallow River Plume of the Northeast Pacific Coastal Temperate Rainforest

Rebecca Whalen[1], Kyra St. Pierre[1,2,3], Colleen Kellogg[3], Ian Giesbrecht[3], Suzanne Tank[4], Lauren Portner[5, 2], Isabelle Desmarais[3], Ryan Hutchins[6], Brian Hunt[2,7]

[1]*Department of Earth and Environmental Sciences, University of Ottawa, Ottawa, Canada*
[2]*Institute for Oceans and Fisheries, University of British Columbia, Vancouver, Canada*
[3]*Hakai Institute, Vancouver, Canada*
[4]*Department of Biological Sciences, University of Alberta, Edmonton, Canada*
[5]*Pacific Salmon Foundation, Vancouver, Canada*
[6]*Department of Chemistry and Biology, Toronto Metropolitan University, Toronto, Canada*
[7]*Department of Earth, Ocean and Atmospheric Sciences, University of British Columbia, Vancouver, Canada*

This chapter is in preparation for submission to *Estuaries and Coasts.*

Abstract

The Northeast Pacific Coastal Temperate Rainforest (NPCTR) spans over 2000 km from Alaska to California and includes thousands of diverse small rain-dominated coastal watersheds that contribute a disproportionate amount of discharge to the Pacific Ocean. Coastal ecosystems receiving these inputs are potential hotspots of biogeochemical transformations but remain understudied. This study examines a river-ocean estuary system on Quadra Island (British Columbia, Canada) to assess how small rain-dominated watershed exports influence coastal microbiology and biogeochemistry. Water samples collected at 0, 15, and 50 cm depth across seven sampling sites in a freshwater plume (0-27.9 PSU) from Hyacinthe Creek into Hyacinthe Bay were analyzed for phosphate, silica, carbon and nitrogen species and isotopes, dissolved organic matter (DOM) composition, and putatively active (RNA) and total (DNA) microbial community structure. Surface samples revealed distinct biogeochemical and microbial signatures distinct from underlying waters, revealing a vertical plume extent of less than 15 centimeters, a scale often overlooked in oceanography. Nutrient and carbon concentrations increased with distance from the river inflow, deviating from conservative mixing and suggesting active reprocessing. Microbial communities exhibited distinct horizontal and vertical structure, supporting a river-to-sea microbial continuum, and revealing taxa that may be disproportionately more active compared to the total community in transitional waters. Salinity, and organic matter were identified as key drivers of coastal microbial community structure. This study highlights that small river plumes may strongly influence biogeochemical cycling and microbial dynamics in rain-dominated NPCTR estuaries at unprecedented scales.

Keywords: Freshwater exports, organic material, nutrients, microbial activity, coastal environments, environmental microbiology

Introduction

Coastal oceans are globally recognized as hotspots for nutrient exchange, carbon cycling, and microbial activity (Maranger et al., 2018; Tee et al., 2021), in large part due to the fact that they receive and integrate water, materials and organisms from both land and the open ocean. This is particularly true in temperate and northern regions of the planet, which receive disproportionately large freshwater influxes (Bianchi et al., 2020), playing a vital role in natural estuarine carbon dynamics (Kim et al., 2021; Yao et al., 2024). Freshwater inputs of organic matter and limiting nutrients, such as nitrogen and iron, to coastal waters drive biological production, supporting marine food webs and reprocessing carbon via microbial uptake and photosynthesis (Anderson et al., 2020; Maranger et al., 2018; Raymond et al., 2013; Vargas et al., 2011). Coastal waters are thus excellent examples of meta-ecosystems, reflecting the interconnectedness of distinct terrestrial and marine ecosystems through flow of energy and materials, and building on a long tradition of estuary science that focuses on these interfaces (Loreau et al., 2003; Menge et al., 2019; St. Pierre et al., 2020; Ward et al., 2020).

The Northeast Pacific Temperate Rainforest (NPCTR) extends from northern California to southeast Alaska along the western coast of North America and receives up to 4000 mm of rain per year, resulting in a massive flux of freshwater to the northeast Pacific Ocean (Bidlack et al., 2021; Giesbrecht et al., 2022). On the British Columbia central and south-central coasts, from Calvert Island to Bute Inlet, rain-dominated watersheds cover 24% of the NPCTR watersheds surface area yet deliver 33% of discharge to the Pacific Ocean (Giesbrecht et al., 2025a). The cumulative freshwater exports in this area – from rain, snow, and glacial melt - are sufficient to affect global ocean circulation, creating the contiguous panarctic Riverine Coastal Domain (RCD), a narrow, shallow, freshwater induced ocean circulation pattern that moves clockwise around North America, affecting oceanic light, nutrient, and carbon dynamics (Carmack et al., 2015). While attention has been paid to the large freshwater plumes along this west coast generated by the large rivers that originate inland of the coastal mountains, such as the Fraser, Columbia, Umpqua, and Eel Rivers, considerably less is known about the dynamics of the small rain-dominated river plumes that define the region (Bidlack et al., 2021; Hunt et al., 2024; St. Pierre et al., 2020).

This discrepancy is due, in part, to the lack of shared frameworks, terminology and instrumentation, with overall differences in scale and ecosystem processes in oceanography and limnology fields (Hunt et al., 2024; Ward et al., 2020). This includes the technical limitations of traditional oceanographic vessels, which are unable to navigate the shallow nearshore coastal environments where the influence of small plumes is highest, along with sampling conventions that may not capture the region of highest freshwater influence. For example, oceanographers often take measurements starting at 5 meter depth, whereas the region of highest freshwater influence of these small plumes is estimated to extend only centimeters to tens of centimeters from

the surface (Hunt et al., 2024). To combat these challenges, it is important to develop new frameworks and further investigate and quantify the interactions (Hunt et al., 2024).

In the present study, we examined dissolved organic matter (DOM), carbon, nutrient (nitrogen, phosphorus and silica) and microbial community (prokaryote and photosynthetic micro-eukaryotes) dynamics from Hyacinthe Creek, a small rain-dominated watershed in the heart of the NCPTR, through a freshwater plume in Hyacinthe Bay, along the coast of Quadra Island, British Columbia, Canada (approx. 50.12° N, 125.23° W). To do so, we combined approaches from both limnology and oceanography to (1) delineate the extent of the plume from a small rain-dominated system; (2) quantify and characterize nutrient concentrations, organic matter, and microbial community composition across the plume; to (3) link microbial community composition to carbon and nutrients at a resolution rarely addressed in the oceanography and limnology fields. We hypothesized that *putatively active microbial community composition, along with biogeochemical trends, will vary significantly across horizontal and vertical salinity gradients in the Hyacinthe Creek–Bay estuary due to fundamental niche shifts caused by increased salinity, with the strongest signals expected in surface waters most directly influenced by freshwater inputs.*

Methodology and Materials

Site Description

Hyacinthe Creek (Figure 2, approx. 50.13° N, 125.25° W) is one of thousands of small, seasonally dynamic, rain-dominated river plumes that flow directly into the Pacific Ocean (Giesbrecht et al., 2025a). It is part of the second largest watershed on Quadra Island (Discovery Islands Forest Conservation Project, 2022), with an area of 15.42 km^2, mean annual precipitation (MAP) of 1699 mm, mean annual air temperature (MAAT) of 8.6°C, lake cover of 0.74%, a max elevation of 591 m (Giesbrecht et al., 2025b), and flowing through a forested watershed underlain by Triassic age basalt (Karmutsen Formation) (Roddick & Woodsworth, 2006). Hyacinthe Creek is part of the Rain Hills-Central (RHC) watershed classification (Giesbrecht et al., 2022, 2025a) (Figure 1), an area characterized by low to moderate relief, productive forests, and moderate organic matter and pH, and high inorganic nutrients, weathering solutes, and buffering capacity relative to other watershed types in the NPCTR (Giesbrecht et al., 2022, 2025a). Hyacinthe Creek flows into Hyacinthe Bay (Figure 2), a shallow, semi-enclosed coastal bay influenced by tidal mixing, estuarine circulation patterns and seasonal productivity (Geyer, 2010). Weather conditions around the sampling period were characterized by increased precipitation and temperatures in the preceding weeks, followed by a brief dry interval immediately preceding sampling (Figure A1).

Field Collection

Sampling was conducted in Hyacinthe Creek (Figure 2) on February 8, 9, and 17, 2022, and in Hyacinthe Bay (Figure 2) from February 16 to 17, 2022. In Hyacinthe Creek (Site 0, -1350 m from the creek mouth, Figure 2), six surface water samples

were collected over three time periods to characterize variation in freshwater quality prior to its discharge into the coastal system. In Hyacinthe Bay, six sites were sampled along a salinity gradient extending from the mouth of the creek into the bay (from 79 m to 780 m from the creek mouth sites 1 through 6, Figure 2) at three depths: surface (0 cm), mid-depth (15 cm), and near-bottom (50 cm). At the site 79 m from the creek mouth, only the top two depths were sampled due to outgoing tidal conditions. From 79 m to 780 m from the creek mouth, samples were collected directly from the side of the rowboat with the use of a peristaltic pump. Water was flushed through the line for 2–3 minutes before sample collection to ensure clean and representative samples.

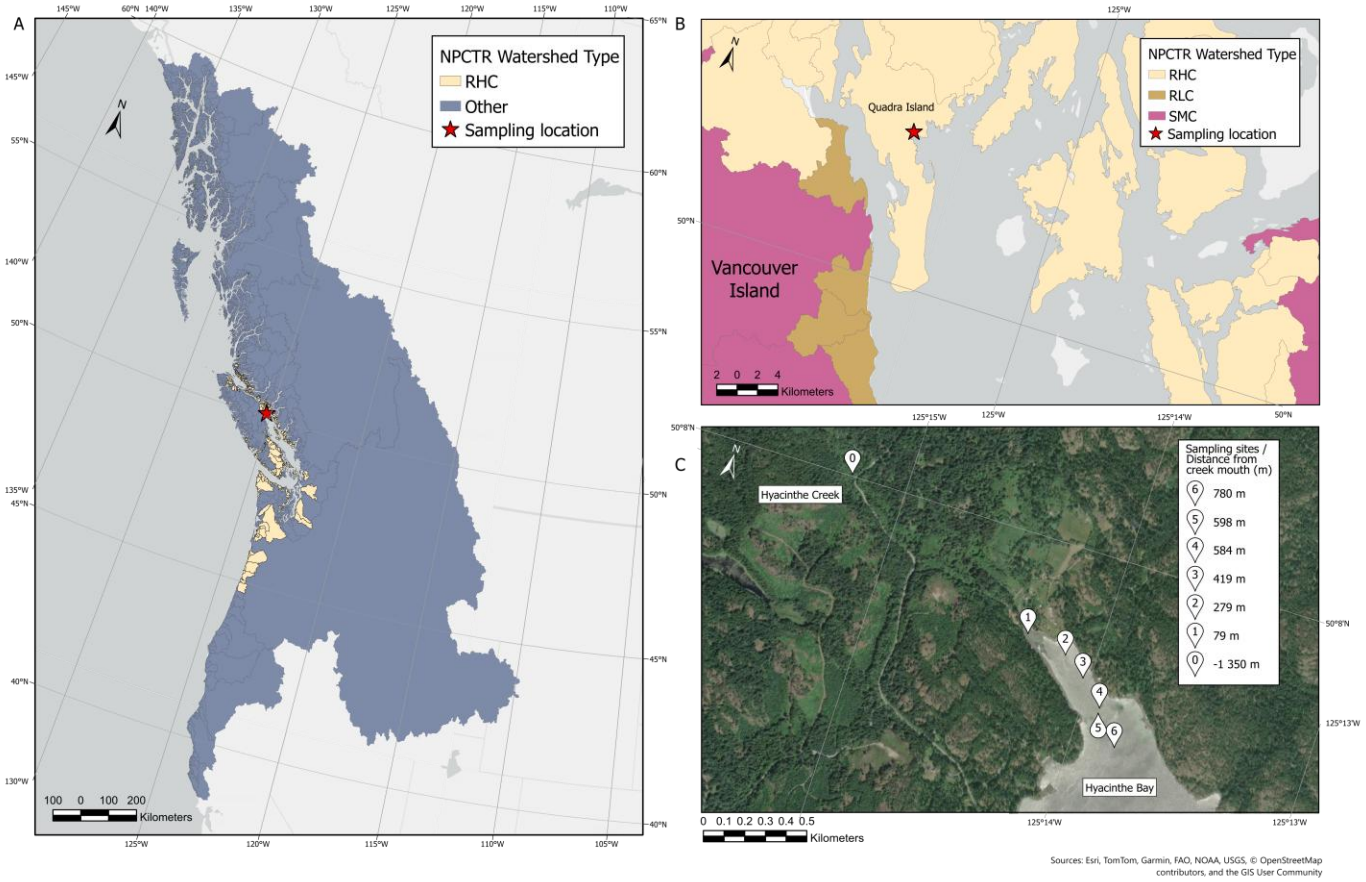

Figure 2: Sampling site locations across nested spatial scales.
(A) The sampling location highlighted with a red star and its watershed type (Rain-hills Central – RHC) highlighted within the 14 diverse Northern Pacific Coastal Temperate Rainforest (NPCTR) watersheds (Gonzalez Arriola et al., 2018). Underlain by a light gray basemap (ESRI et al., 2011). (B) Zoomed in view of Quadra Island with the sampling location highlighted with a red star and the RHC, RLC, and SMC watershed types highlighted (Gonzalez Arriola et al., 2018). Underlain by a light gray basemap (ESRI et al., 2011). (C) Detailed view of the Hyacinthe Creek–Bay river plume transect with sampling sites (0–6) marked by distance from the creek mouth (m). Distances were calculated using the ArcGIS Pro measure tool (ESRI, 2025a). Underlain by an imagery basemap (ESRI, 2009).

Clean water sampling vessels (carboys, syringes, and centrifuge tubes) were rinsed three times with sample water prior to filling. Approximately 6–7 L of water were collected per site. Water samples for total dissolved nitrogen (TDN), phosphate (PO_4^{3-}), silica (SiO_2), dissolved organic carbon (DOC), ammonium (NH_4^+), and combined nitrate-nitrite ($NO_3^- + NO_2^-$, hereafter simplified to NO_3^-) samples were filtered directly in the field through 0.45 µm polyethylsulfonate (PES) filters. Bulk water

samples for total nitrogen (TN) and total phosphorous (TP) were collected in 50-mL centrifuge tubes. Bulk water samples for microbial community composition and particulate carbon/nutrient concentrations were stored in bleach-soaked and MilliQ-rinsed 2 L bottles. All samples were kept cool and out of the light until further processing.

Physical characteristics of the plume were mapped using a YSI ProDSS sonde. Briefly, the sonde was lowered to each sampling depth (0, 15, and 50 cm) at 48 locations horizontally across the plume to record physical parameters, including temperature, specific conductivity, and salinity.

Sample processing and preservation

Initial processing of nutrient and carbon sample concentrations occurred at the Hakai Quadra Island Ecological Observatory before being sent off to external laboratories for further analysis using established protocols (Appendix B, Table 2). TN, TP, TDP, TDN, NH_4^+, PO_4^{3-}, SiO_2, and NO_3^- samples were stored in the freezer. Samples for TP, TDP, NH_4^+, TN, TDN were sent to the University of Alberta's Biogeochemical Analytical Service Laboratory (Edmonton, AB, Canada), while samples for SiO_2, PO_4, and NO_3^- were sent to the University of British Columbia's Marine Zooplankton and Micronekton Laboratory (Vancouver, BC, Canada) for analysis. DOC and $\delta^{13}C$ samples were preserved with 7.5M H_3PO_4 for both freshwater and marine samples and refrigerated until analysis using a total organic carbon analyzer coupled to a mass spectrometer at the Ján Veizer Stable Isotope Laboratory (University of Ottawa, Ottawa, ON, Canada). Samples for particulate organic carbon and nitrogen (POC, PN) concentrations and stable isotope signatures ($\delta^{13}C$-POC, $\delta^{15}N$-PN) were filtered through muffled 0.7 µm GF/F filters. The POC filters were acidified with 200µL of 6M HCl to release traces of inorganic carbon. Samples were then frozen until further analysis using an elemental analyzer–isotope ratio mass spectrometry (EA–IRMS) at the University of California Davis Stable Isotope Facility (Davis, California, USA).

Fourier Transform Ion Cyclotron Resonance Mass Spectrometry (FT-ICR-MS)

Samples for dissolved organic matter (DOM) characterization were analyzed by Fourier Transform Ion Cyclotron Resonance Mass Spectrometry (FT-ICR-MS) at the Trent University Water Quality Centre (Peterborough, Canada). Processing for the resulting formulae followed the protocol outlined in (Orlova et al., 2024). Classification of compound classes were calculated following the same protocol for oxygen to carbon (O/C) and hydrogen to oxygen ratios (H/C), and the modified aromaticity index (AI_{mod})(Eq. 1), reflecting the carbon unsaturated bond density in each formula(Koch & Dittmar, 2006; Qi et al., 2022; Ren et al., 2024). This allowed for classification of aliphatics ($H/C \geq 1.5$), aromatics ($0.5 \leq AI_{mod} < 0.67$), condensed aromatics ($AI_{mod} \geq 0.67$), and low-O unsaturated ($H/C < 1.5$, $AI_{mod} < 0.5$, and $O/C \leq 0.5$) and high-O unsaturated compounds ($H/C < 1.5$, $AI_{mod} < 0.5$, and $O/C > 0.5$) (Koch & Dittmar, 2006; Orlova et al., 2024; Qi et al., 2022; Ren et al., 2024).

Microbial Community Profiling Using Amplicon Sequencing

Nucleic Acid Extraction

Bulk water samples for microbial community analysis were filtered through 0.2 µm Sterivex filters at the Hakai Institute Quadra Island Ecological Conservatory Marna Lab within 4 hours of sample collection (Kellogg, 2024). Sample filters were frozen immediately at -70°C until nucleic acid extraction. Nucleic acids were extracted using a Macherey Nagel NucleoSpin RNA mini kit paired with the RNA/DNA buffer set to extract both DNA and RNA in parallel. Manufacturer instructions were generally followed, with the following modifications. Samples were lysed enzymatically within the Sterivex capsules by adding 500uL 1mg/ml lysozyme in TE buffer to each capsule, placing the Sterivexes into sterile 50mL conical tubes, and then incubating, while rotating, for 10 minutes at 37°C. Then, scaled up from the manufacturers protocol to ensure the entire sterivex filter was immersed, 1300 µL buffer RA1 and 18 µL betamercaptoethanol was added to each filter and vortexed in a fume hood. The betamercaptoethanol was added at 1/100 of the total volume of lysozyme + buffer RA1, as per the manufacturer recommendations. After vortexing, lysate was then removed from the Sterivex. This was done by placing a 5 mL screw cap tube, pre-loaded with 0.7 g of 400 µm glass beads, into a 50 mL tube using forceps. Sterivex units were then inverted and placed into the 50 mL tubes so that the Sterivex inlet was in the 5 mL tube and centrifuged at 4,000 x g for 1 minute, collected the lysate into the 5 mL tube. The sterivex and 5 mL tubes were removed from the 50 mL tube, the Sterivex discarded and the 5 mL tube capped and vortexed for 5 minutes for a final mechanical lysis. Following this, the lysate was transferred to a NucleoSpin Filter tube in 600 µL aliquots, centrifuged at 11,000g x 1 min, until all lysate was passed through the column, transferring the flow-through (sample) into a new 5 mL tube after each spin. The RNA binding conditions of the sample was then adjusted with a 1:1 ratio of 70% ethanol (1800 µL) and vortexed and gently pipet-mixed. After this, the sample was loaded onto a NucleoSpin RNA Column placed in a Collection Tube in 600 µL aliquots, spun at 10,000g for 30 s, disposing of the flow-through after each spin, until all the sample was passed through the RNA column. From here forward, the manufacturer's instructions were followed, skipping the DNAase step. Once the RNA and DNA extractions were complete, the RNA samples were treated with DNase using the Invitrogen Turbo DNA-*free* kit. RNA was then converted to cDNA using the Invitrogen Superscript III First-Strand Synthesis System kit.

Amplicon Sequencing and Bioinformatics

The V4-V5 region of the 16S rRNA gene was amplified from DNA and cDNA and sequenced to generate microbial community profiles. A fusion primer approach (Kellogg et al., 2024) was used to prepare the 16S rRNA gene amplicon libraries using the 515F (5'-GTGYCAGCMGCCGCGGTAA-3') and 926R (5'-CCGYCAATTYMTTTRAGTTT-3') primer pair. The amplicon library was sequenced on an Illumina MiSeq (600 cycle V3 kit) and processed using the QIIME2 v. 2022.8 platform. Briefly, primers were trimmed from sequence data using the cutadapt QIIME2 plugin using the default settings and sequences were denoised and amplicon sequence variants (ASV) determined using the DADA2 QIIME2 plugin using following settings (--p-trunc-len-f 280, --p-trim-left-r 25, --p-trunc-len-r 160, --p-max-ee-f 3, and --p-max-ee-r 5). Rare ASVs were removed

(<0.1% of the average read depth of the library) to mitigate sequencing error. Taxonomic classification was initially conducted using the QIIME2 Naïve Bayes classifier (Bokulich et al., 2018) trained on SILVA v138.1 database (Chuvochina et al., 2026) Mitochondrial and chloroplast sequences were removed, and the remaining sequences constituted the prokaryotic dataset. Chloroplast sequences were extracted and further classified using a classifier trained on the PR2 v5 database (Guillou et al., 2013) to provide a look at the photosynthetic microbial eukaryotes. Note that photosynthetic dinoflagellates are not captured using this amplicon and thus are not represented in this dataset, despite comprising a potentially critical component of marine phytoplankton communities (McNichol et al., 2025).

Data Processing

Visualization of the salinity gradient from the 48 points sampled across the plume was done in ArcGISPro (ESRI, 2025a) using three-dimensional (3D) interpolation. A polygon feature class was created manually around the plume and sampling area. A model was then created in a new toolbox, and the (1) *Empirical Bayesian Kriging 3D (ESRI, 2025b)* and (2) *GA Layer To NetCDF (ESRI, 2025)* tools were added consecutively with the plume salinity mapping data file as an input (elevation as depth (cm)) to (1), and the resulting interpolated surface as input to (2), with voxel clipping options set to the created plume polygon feature class. Once generated, the file was added to a local scene, and displayed in a layout, with an additional longitudinal cross-section generated using the splice tool.

The resulting biogeochemical datasets (nutrient and carbon concentrations/compositions and ratios, FT-ICR-MS results, microbial ASVs, taxonomy, and metadata CVSs) were imported into RStudio (Posit team, 2025) for visualization using tidyverse (Wickham et al., 2019), vegan (Jari Oksanen et al., 2025), patchwork (Pedersen, 2025), adespatial (Dray S et al., 2025), mgcv (Wood, 2011), ggforce (Pedersen, 2025), ggrepel (Slowikowski, 2024), and ggnewscale (Campitelli, 2025) packages. The amplicon sequencing dataset presents a series of DNA and RNA (i.e. cDNA) sequencing counts for a microbial ID at each depth and site/distance. Each ID corresponds to a microbial identity as defined in a taxonomy key, which were then attributed according to their taxonomic order. Duplicate IDs were merged to represent a single order, and relative abundances were calculated for all prokaryotic (i.e. microbes, n = 859) and photosynthetic microeukaryotic (i.e. plastids, n = 91) orders, then filtered for the top 15 orders by relative abundance. Prokaryotic and photosynthetic eukaryotic relative abundances and nutrient and organic matter measurements matrices are identified as the multivariate response variables for redundancy analysis (RDA). Hellinger transformation (Borcard et al., 2011; Legendre & Gallagher, 2001) was applied to community data to reduce dominance effects. Redundancy analysis (RDA) (Borcard et al., 2011; Legendre & Gallagher, 2001) was performed for DNA and RNA relative abundances for both photosynthetic eukaryotes and prokaryotes separately to draw connections between community composition (DNA and RNA) and environmental variables. A forward selection of the environmental variables was performed, using permutations (999 permutations, $\alpha = 0.05$) to highlight significant environmental drivers. R scripts were

developed and edited using RStudio for data processing and visualization, with assistance from the ChatGPT language model (OpenAI, 2025) to improve code efficiency, formatting, and aesthetic presentation. All analytical decisions, data handling, and interpretations were performed by the authors.

Results

Salinity gradient and plume extent

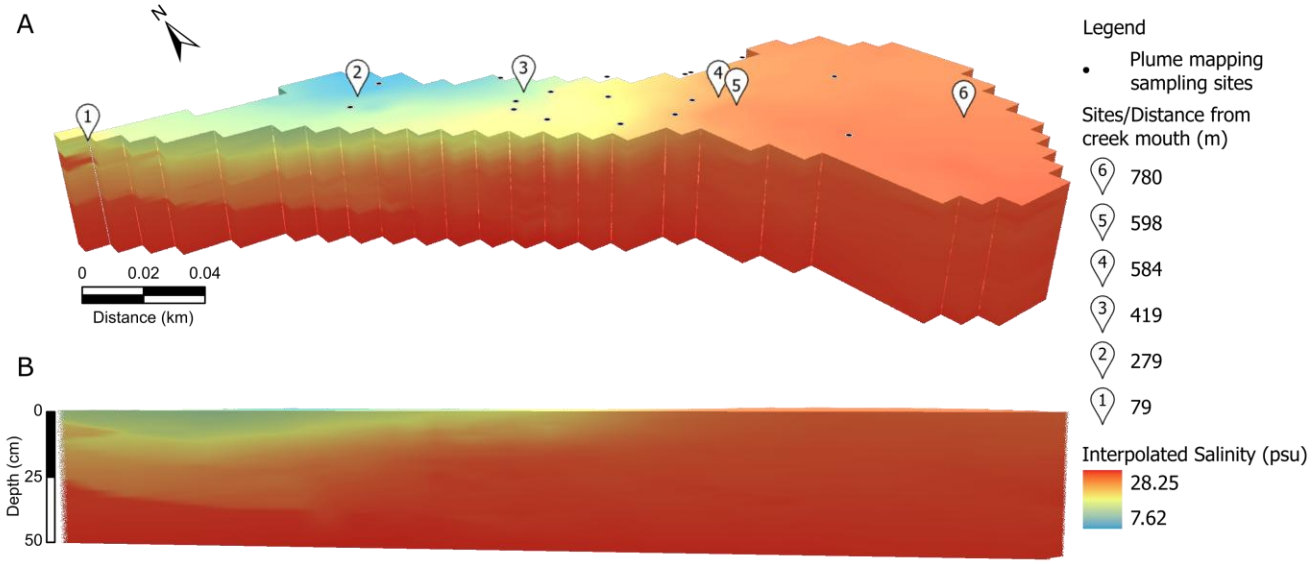

Figure 3: Three-dimensional salinity reconstruction of the estuarine plume.
(A) Oblique Three-dimensional (3D) view of interpolated salinity (PSU) using 3D Empirical Bayesian Kriging with a vertical exaggeration of 2.44, highlighting horizontal and vertical structure of the plume, with warmer colors indicating higher salinity and cooler colors indicating fresher, plume-influenced waters. Sampling locations used for biogeochemical and microbial analyses are shown as white pins, while black points indicate additional stations used for high-resolution plume mapping. (B) Longitudinal vertical section extracted along the main axis of the estuary highlighting landward–seaward salinity gradients and stratification over depth.

Surface salinity across the plume ranged from 7.62 to 28.25 PSU (Figure 3; Figure A2), generally increasing with increasing distance from the creek mouth, though the lowest salinity (7.62 PSU) was located not at the site 79 m from the creek mouth, but rather, 279 m north of the creek mouth. Low salinity measurements were restricted to the surface of the water column (0 cm), increasing to a mean salinity of 24.5 PSU (SD = 3.1) at 15 cm, then to a mean of 27.7 PSU (SD = 0.3) at 50 cm. There was minimal difference between 15 and 50 cm, with less saline conditions around 270 m north of the creek mouth at 15 cm which disappeared by 50 cm.

Organic Matter and Nutrient Dynamics

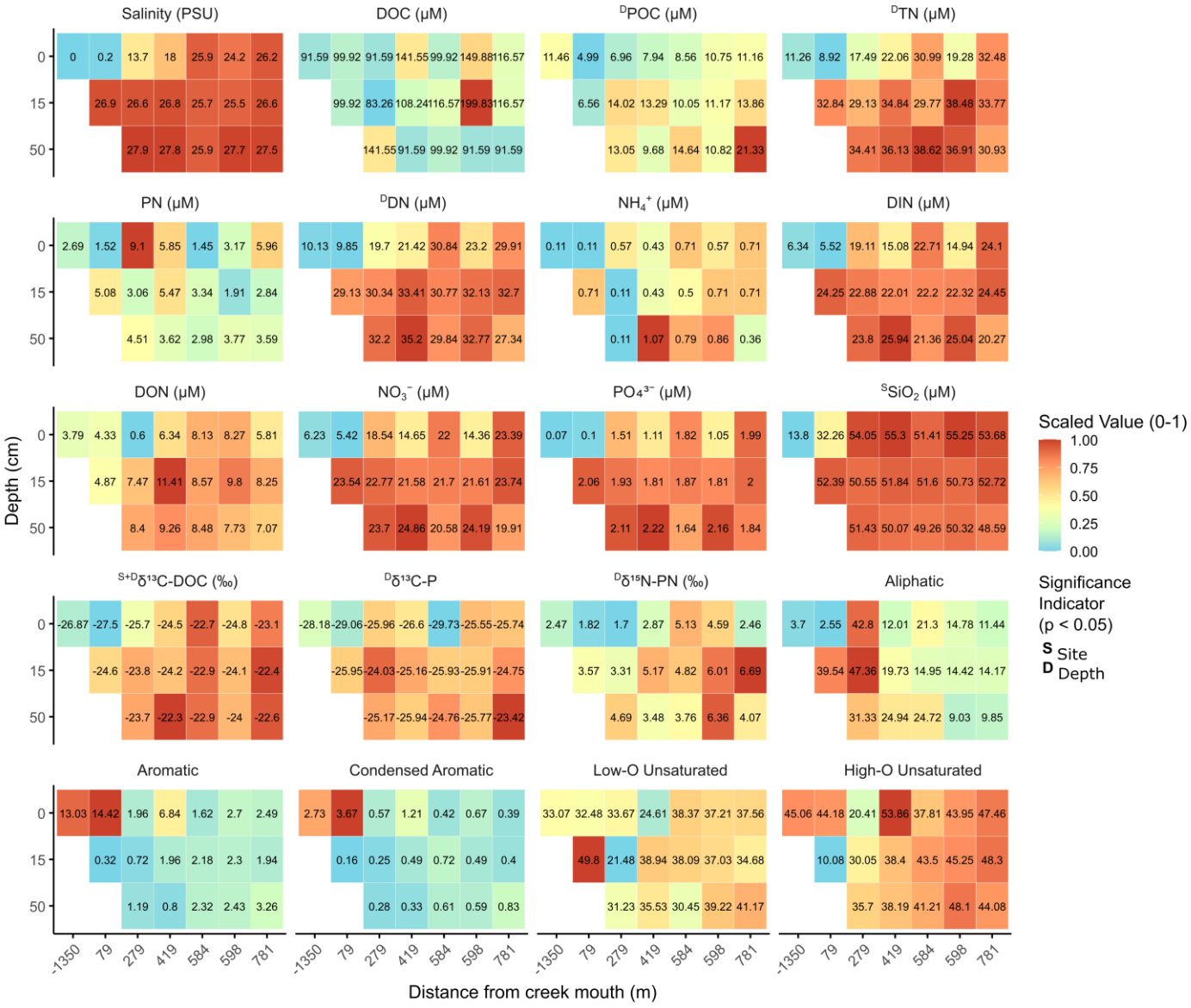

Figure 4: Vertical and Horizontal Distributions of Nutrients, Carbon, and Dissolved Organic Matter Compound Classes from Hyacinthe Creek (-1350 m from creek mouth) and across the plume (distance > 0 m). Heatmap displaying salinity (practical salinity units), carbon (DOC, POC) and nutrient (TN, PN, DIN, NO_3^-, NH_4^+, DON, PO_4^{3-}, SiO_2) concentrations (μM), stable isotope (δ^{13}C-DOC, δ^{13}C-POC, δ^{15}N-PN) signatures (‰), and DOM compound classes (aliphatic, aromatic, condensed aromatic, low-O and high-O unsaturated) by depth (0, 15, 50 cm) and distance from creek mouth (-1 350 to 781 m). The value bars and colours are standardized by parameter, with colouring reflecting a scale of 0-1 of the entire range of values. ANOVA test significance indicators (where $p < 0.05$) are bolded with superscripts ($^{\mathbf{S}}$ = significant by site/distance; $^{\mathbf{D}}$ = significant by depth).

Nutrient and carbon concentrations, stable isotope signatures, and relative proportion of DOM compound classes varied across the plume (i.e., distance from the creek mouth) and with depth across the plume (Figure 4). TN and DN concentrations increased significantly with depth (p = 0.012 and 0.019, respectively) (Table A3), ranging from 8.92 to 38.62 μM, and 9.82 to 35.2 μM, respectively (Table A4). In contrast, variations in PN, NH_4^+, DIN, NO_3^-, and DON were insignificant (p = 0.667, 0.839, 0.092, 0.078 and 0.060, respectively) (Table A3), with ranges of 1.45 to 9.10 μM, 0.11 to 1.07 μM, 5.52 to 25.92 μM,

5.42 to 24.86 μM and 0.60 to 11.41, respectively (Table A4). δ^{15}N-PN increased significantly by depth ($p = 0.047$) (Table A3), ranging from 1.70 to 6.69 ‰ (Table A4). SiO_2 increased significantly with increasing distance ($p = 0.002$) (Table A3) with a range of 13.80 to 55.30 μM (Table A4). PO_4^{3-} was found insignificant despite increasing from and 0.07 to 2.22 μM (Table A4). DOC concentrations did not vary systematically with distance or depth (range = 83.29 to 199.83 μM) (Table A3; Table A4), while POC concentrations only increased significantly depth ($p = 0.041$, 4.99 to 21.33 μM) (Table A3; Table A4). δ^{13}C-DOC increased significantly with distance and depth ($p = 0.011$, 0.048, respectively) (Table A3), ranging from -27.50 to -22.30 ‰ (Table A4), while δ^{13}C-POC increased significantly by only depth ($p = 0.033$, -29.73 to -23.42 ‰ ; Table A3, Table A4). Condensed aromatic and aromatic compounds decreased insignificantly (Table A3), ranging from 0.17 to 3.67 and 0.32 to 14.42, respectively (Table A4). High-O and low-O unsaturated compounds and aliphatics exhibited potential hotspots/hot moments at various distances from the creek mouth (79 m, 15 cm depth and 279 m, 0 cm and 15 cm depth), ultimately showing variation along gradients (despite insignificance) (Table A3), with a range of 10.08 to 53.86, 21.48 to 49.80, and 2.55 to 47.36 relative proportions, respectively (Table A4). CHON percent relative abundance increased significantly along the plume ($p = 0.005$), ranging from 0.63 to 3.10 %, whereas C/N DOM ratios decreased significantly ($p < 0.001$), ranging from 14.79 to 11.65 (Table A5). The ratios DIN:P decrease significantly along distance ($p=0.022$) (Table A3), ranging from 90.04 to 11.03 (Table A4), dropping below the nitrogen limitation ratio of 16:1 (Figure A3). Along the salinity gradient, DOC, POC, PN, and their stable isotopes (δ^{13}C-DOC, δ^{13}C-POC, δ^{15}N-PN) deviate from the conservative mixing line (Figure A4).

Microbial Community Dynamics

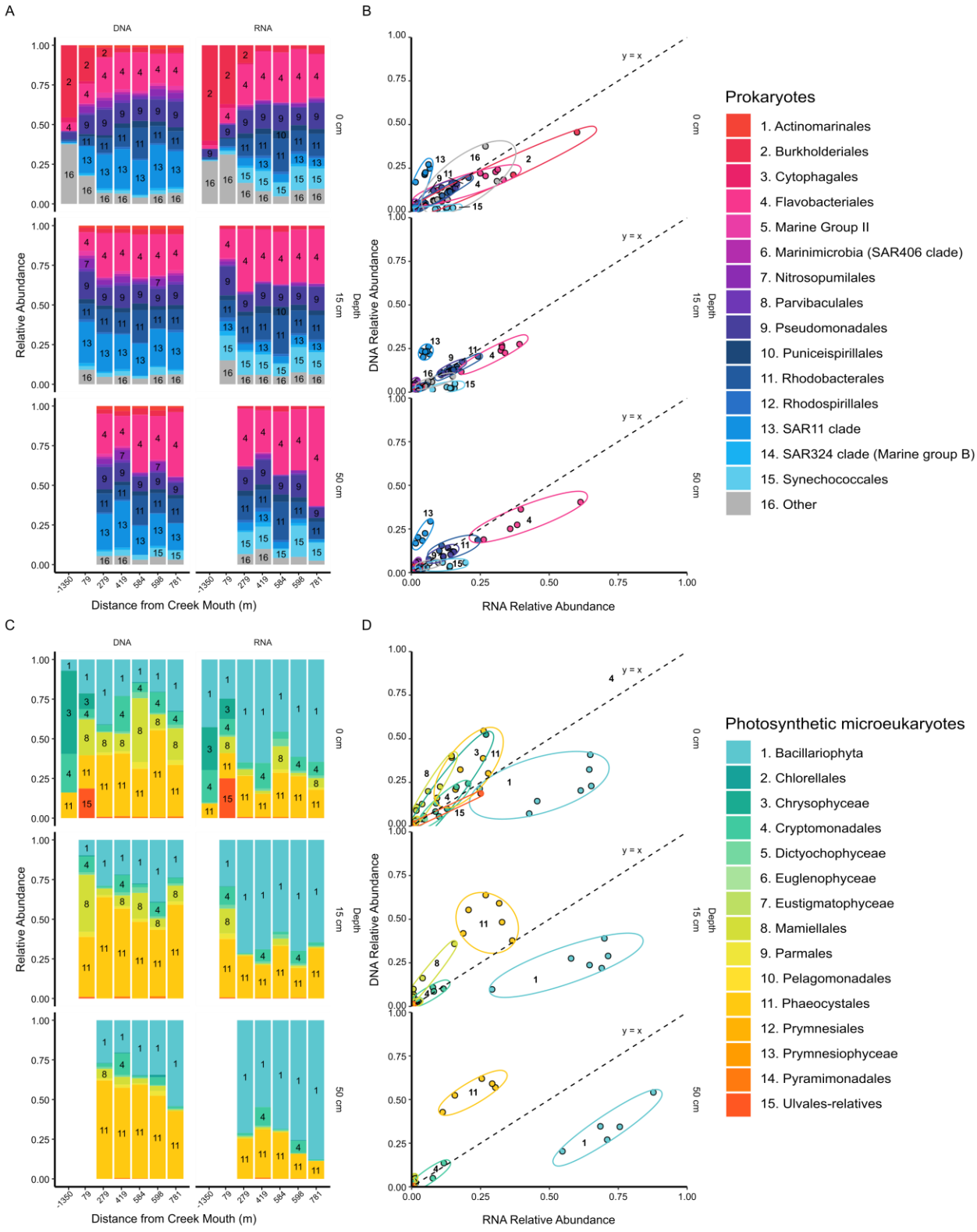

Figure 5: Microbial Community Composition by distance from creek mouth (m) and depth (cm).
Relative abundances of dominant (top 15) prokaryotic (A) and photosynthetic microeukaryotic (C) orders based on DNA and RNA at each depth and distance from the creek mouth (m). Scatterplots comparing dominant (top 15) prokaryotic (B) and photosynthetic microeukaryotic (D) DNA:RNA relative abundance. Colours represent prokaryotic (top) and photosynthetic microeukaryotic (bottom) top 15 orders.

Prokaryotes

The relative abundance of prokaryotic sequences (Figure 5A; Table A6) indicated distinct dominant orders within the top 15 orders for both DNA and RNA. DNA and RNA samples were dominated by *Flavobacteriales, Pseudomonadales, Rhodobacterales,* and *Burkholderiales,* with *SAR11 clade* dominating DNA exclusively and *Synechococcales* for RNA exclusively. Notably, *Burkholderiales* was highly abundant for both RNA and DNA for the sites with the strongest freshwater influence (-1350, 79, and 279 m) but declined rapidly seawards (Figure 5). Two-way ANOVA results support these trends, showing significant variability ($p < 0.05$) with distance from the creek mouth or depth for ten of the 15 orders (Table A7). Significant effects are observed for relative abundances of *Burkholderiales* ($p < 0.001$ (DNA), 0.004 (RNA)), *Cytophagales* ($p > 0.001$ (DNA), 0.010 (RNA)), *Marinimicrobia (SAR406 clade)* ($p = 0.045$ (DNA)), *Nitrosopumilales* ($p = 0.004$ (DNA)), *Parvibaculales* ($p = 0.048$ (DNA)), *Puniceispirillales* ($p = 0.012$ (DNA), 0.001 (RNA)), *Rhodobacterales* ($p > 0.001$ (DNA, RNA)), *SAR11* ($p = 0.010$ (DNA)), *SAR324 clade (Marine group B)* ($p = 0.012$ (DNA)), and *Synechococcales* ($p = 0.035$ (DNA), 0.038 (RNA)) with increasing distance from the creek mouth (Table A7). Depth effects were sparing, with only *Marinimicrobia (SAR406 clade)* ($p = 0.031$ (DNA)), *Synechococcales* ($p = 0.003$ (DNA)), and *Rhodobacterales* ($p = 0.016$ (RNA)) varying significantly with depth (Table A7). The remaining orders showed no statistical response to either depth or site (Table A7). The ratio of RNA to DNA (RNA:DNA) (Figure 5B) revealed that several orders deviated from a 1:1 relationship ($y = x$) between relative sequence abundances, indicating differences between putative active and present microbes (Figure 5B). Through linear mixed modeling (Table A8), 11 of 15 orders exhibited significant deviations from the 1:1 RNA:DNA line ($p < 0.05$). Of these 11 orders, *Actinomarinales, Marine Group II, Marinimicrobia (SAR406 clade), Nitrosopumilales, Parvibaculales,* and the *SAR11 clade* (all $p < 0.001$) were significantly more abundant than active, whereas *Flavobacteriales* ($p = 0.001$), *Puniceispirillales* ($p < 0.001$), *Rhodobacterales* ($p = 0.013$), *Rhodospirillales* ($p = 0.011$), and *Synechococcales* ($p < 0.001$) were significantly more active than abundant (Table A8). Beta Diversity indices (β) comparing the freshwater site (site 0, -1350 m from the creek mouth) and the most marine site (site 6, 789 m from the creek mouth) show taxonomic dissimilarity values of 0.896 for DNA and 0.849 for RNA.

Photosynthetic microeukaryotes

Similarly, photosynthetic micro-eukaryotic communities were dominated (Figure 5C; Table A6) by the orders *Phaeocystales, Bacillariophyta, Mamiellales, Chrysophyceae,* and *Cryptomonadales*. Two-way ANOVAs highlight significant variations ($p < 0.05$) for RNA and DNA relative abundances for six of 15 photosynthetic microeukaryotic orders along the salinity gradients (Table A7). Those which varied significantly with increasing distance from the creek mouth include *Chrysophyceae* ($p < 0.001$ (DNA), 0.001 (RNA)), *Cryptomonadales* ($p = 0.001$ (DNA, RNA)), *Baccilariophyta* (0.004 (RNA)), *Mamiellales* (0.037 (RNA)), and *Pyramimonadales* ($p = 0.009$ (RNA)) (Table A7). In contrast, orders varying significantly with depth include

Cryptomonadales ($p = 0.041$ (DNA), 0.043 (RNA)) and *Phaeocystales* ($p = 0.024$ (DNA)) (Table A7). There were notable discrepancies between putative activity and abundance for five of the 15 orders (Figure 5; Table A8). Of these five, *Bacillariophyta* was more active than abundant ($p < 0.001$), whereas *Chlorellales* ($p = 0.001$), *Mamiellales* ($p = 0.001$), *Parmales* (0.002), and *Phaeocystales* ($p < 0.001$) were more abundant than active (Table A8). Beta Diversity indices (β) comparing the freshwater site (site 0, -1350 m from the creek mouth) and the most marine site (site 6, 789 m from the creek mouth) show taxonomic dissimilarity values of 0.9875 for DNA and 0.9753 for RNA.

Biogeochemical drivers of putatively active microbes across a small freshwater plume

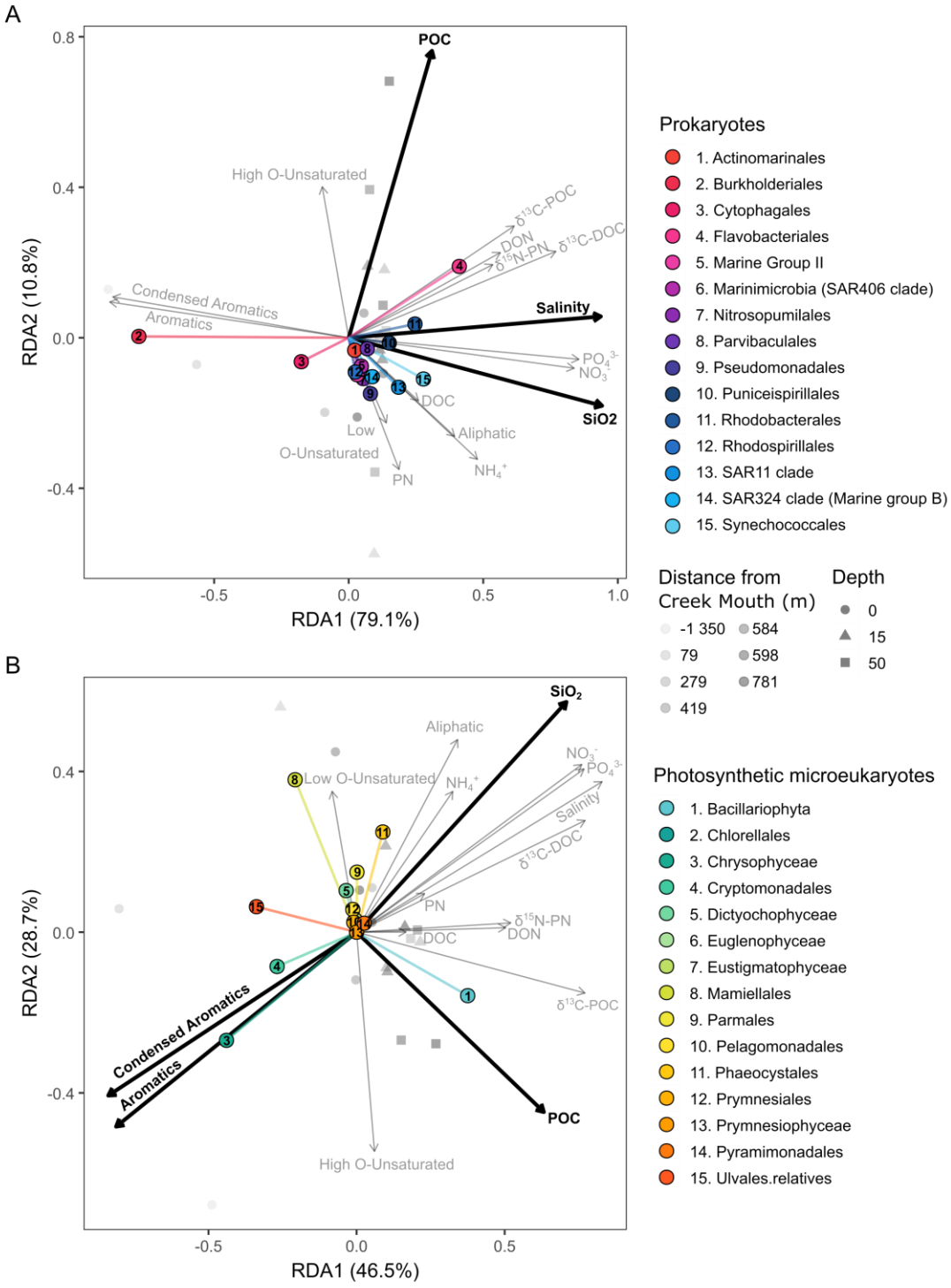

Figure 6: Environmental drivers of putatively active (A) prokaryotes (based on 16S rRNA) and (B) photosynthetic microeukaryote communities (based on plastid 16S rRNA).
Redundancy analyses of putatively active microbes by proxy of RNA relative abundance constrained by organic matter (DOC, POC, δ^{13}C-DOC, δ^{13}C-POC, aliphatics, aromatics, condensed aromatics, low-O unsaturated, and high-O unsaturated compounds), nutrient (δ^{15}N, PN, DON, NO_3^-, NH_4^+, PO_4^{3-}, SiO_2) and physical (salinity) parameters with axes showing the cumulative percentage of variance explained. Coloured points represent dominant prokaryotic and photosynthetic eukaryotic orders, grey symbols indicate individual samples faceted by depth and distance from creek mouth, and black vectors highlighting environmental variables identified by forward selection in bold. Calculated concentrations or redundant parameters (TOC and DIN) were excluded from this analysis.

The distribution of putatively active prokaryotes was reflective of strong gradients in salinity, SiO_2, aromatic and condensed aromatic compounds, PO_4^{3-}, NO_3^-, and δ^{13}C-DOC that collectively explained 79.1% (RDA1) of variance in community composition (Table A9). RDA2 largely reflected variability in organic matter characteristics, including POC, PN, and NH_4^+ concentrations, aliphatic and high-O unsaturated compounds, and δ^{13}C-POC signatures, accounting for 10.8% of the total variance (Table A9). *Burkholderiales* and *Cytophagales* were positively related to aromatic and condensed aromatic compounds but negatively related to salinity and SiO_2 concentrations, whereas *Flavobacteriales, Rhodobacterales* and *Rhodospirillales* were positively related with salinity and SiO_2 concentrations (Figure 6). The distribution of putatively active photosynthetic microeukaryotes reflected strong gradients in salinity, condensed aromatic compounds, PO_4^{3-} and NO_3^- concentrations, and δ^{13}C-DOC and δ^{13}C-POC signatures, cumulatively accounting for 46.5% of variance (RDA1) in the photosynthetic microeukaryote community composition (Table A9). RDA2 reflects variability of SiO_2 and POC concentrations, and high-O unsaturated and aliphatic compounds, explaining 28.7% of variance in community activity (Table A9). *Bacillariophyta* were positively related to higher POC concentrations and high-O unsaturated compounds, whereas *Chrysophyceae*, and *Dictyochophyceae* were related to aromatic and condensed aromatics compounds and lower salinity (Figure 6). *Mamiellales* and *Ulvales relatives*, project negatively with RDA1, but positively with RDA2, correlating with aliphatic and low-O unsaturated compounds (Figure 6). While differing in the microbial groups analysed (prokaryotes vs photosynthetic microeukaryotes), Axis 1 and 2 in both RDAs reflect similar gradients, with RDA1 representing a salinity gradient, and RDA2 representing an organic matter gradient (Figure 6).

Discussion

Vertical and horizontal extents of a small freshwater plume in the NPCTR

The freshwater plume is largely restricted to the very upper surface level (<15 cm) of the water column (Figure 3). To the best of our knowledge, this is the first time that the depth of an exceedingly small plume has been explicitly evaluated. This thin surface layer (Figure 3) aligns with existing estimates of the hypothesized extent of small rain-dominated plumes from NPCTR watersheds, extending only tens of centimeters and dissipating within 0.1 to 3 km (Basdurak et al., 2020; Hunt et al., 2024). This plume extent is very shallow compared to the large plumes that currently form the basis of our understanding of the waters at the interface of lands and oceans (Horner-Devine et al., 2015; O'Donnell et al., 2008). Using this high resolution, sub-meter sampling scheme, we captured strong horizontal and vertical salinity and biogeochemical gradients from Hyacinthe Creek into Hyacinthe Bay at much smaller scales but similar to those observed in these larger systems (F. Chen & MacDonald, 2006; Dagg et al., 2004; Horner-Devine et al., 2015). Though estuarine studies have long-emphasized cross-realm matter flows

and connectivity, it is often at scales far larger than those identified here (Hunt et al., 2024; Ward et al., 2020). These findings highlight the need for studying these small river-ocean ecosystems through a much more refined lens (Loreau et al., 2003).

Nutrient and carbon dynamics along the land-to-ocean continuum across a small rain-dominated plume

Freshwater can be an important vector for allochthonous nutrients and organic matter to coastal oceans (Anderson et al., 2020; Raymond et al., 2013). The measured concentrations of key inorganic nutrients (NO_3^-, SiO_2, and PO_4^{3-}) sat within the expected range of < 2 μM to > 10 μM [NO_3^-], < 0.1 μM [PO_4^{3-}], and > 40 μM [$Si(OH)_4$] for the NPCTR region (Hunt et al., 2024). Although nutrient and carbon concentrations varied with increasing distance from the creek mouth or depth (i.e., TN, DN, SiO_2, POC, Figure 4), these concentrations were often lower in freshwater than in the receiving marine environment, suggesting dilution rather than enhancement of these coastal pools. This has been previously observed for inorganic nutrients (NO_3^-, SiO_2, and PO_4^{3-}) further north in the NPCTR (St. Pierre et al. 2021).

Contrary to other regions of the NPCTR where freshwaters are important sources of DOC and DON to the coastal Pacific Ocean (McNicol et al., 2019; 2023), we find that that DOC, DON concentrations were relatively consistent across the plume. This may be reflective of the fact that Hyacinthe Creek is a Rain-Hills Central type watershed (Giesbrecht et al. 2022), which is generally poorly represented in our conceptual understanding of the NPCTR. The focal NPCTR estuaries studied to date receive discharge from watersheds with very heavy rainfall (~4000 mm yr^{-1}), with deep, organic-rich soils underlain by plutonic bedrock (McNicol et al., 2023; St. Pierre et al., 2020, 2022). In comparison, the Hyacinthe Creek watershed receives considerably less rainfall (1699 mm annually) within the rain shadow created by the mountains of Vancouver Island (Giesbrecht et al., 2022, 2025a) and is underlain by Triassic aged basalt (Upper Karmutsen Formation) (Roddick & Woodsworth, 2006). While geology may have restricted the accumulation of organic-rich soils that are the ultimate source of most terrestrial DOM, it was found that climate and topography are the primary drivers for lower DOC and DON concentrations in this region (explaining > 80% of mean concentrations); thus climate and topographic variation is the likely factor behind these results (Giesbrecht et al., 2022, 2025a).

A significant decrease in DIN:TP with distance and depth (Figure A3, Table A3), supports a shift in potential nutrient limitation from phosphorous to nitrogen limitation seaward, consistent with existing literature, potentially impacting the metabolic potential of microbial species along the plume (Howarth & Marino, 2006; James et al., 2015; Moore et al., 2013; Ngatia et al., 2019; Ptacnik et al., 2010). Deviations from conservative mixing (Figure A4) demonstrate that simple water column mixing is likely not the sole factor affecting nutrient and carbon concentrations and composition of small rain-dominated river plumes. Enhanced microbial reprocessing and remineralization of terrestrial materials likely affect the biogeochemistry of these coastal regions (Fry, 2002; Loder & Reichard, 1981; Plont et al., 2023). This variability is, however,

not linear, and suggests that hotspots and hot moments exist across these plumes at spatial and temporal scales (Ward et al. 2020).

Microbial responses to physical and biogeochemical gradients over small scales

We observed significant variation in the community composition of present and putatively active microbial orders, both prokaryotic and photosynthetic microeukaryotic, along horizontal and vertical gradients (Figure 5). Prokaryotic and photosynthetic microeukaryotic top orders demonstrated clear horizontal and vertical structures with several key taxa (e.g., *Burkholderiales, Cytophagales, Marinimicrobia (SAR406 clade), Nitrosopumilales, Parvibaculales, Puniceispirillales, Rhodobacterales, SAR11 clade, SAR324 clade (Marine group B)*, *Synechococcales, Chrysophyceae, Cryptomonadales, Baccilariophyta, Mamiellales, Pyramimonadales* and Phaeocystales) increasing or decreasing significantly ($p < 0.05$) throughout the plume. These findings, along with high beta diversity indices (β), support the existence of a microbial river-to-sea continuum, where taxonomic diversity is positively correlated with increasing salinity (i.e., high taxonomic diversity between freshwaters and marine ecosystems) (Tee et al., 2021). These results indicate little overlap in community composition between sites, an observation that is consistent with changing fundamental niches and osmoregulatory strategies as salinity increases (Sipler et al., 2017; Tee et al., 2021; Wang et al., 2021; Zeglin, 2015). This study supports that freshwater orders fade seaward while marine and plume-adapted taxa dominate biogeochemical processes in these transitional waters and in processing allochthonous subsidies (S. R. Anderson & Harvey, 2022; Tee et al., 2021; Wang et al., 2021).

DNA- and RNA-based patterns, used here as proxies for the relative abundances of total and putatively active microbial taxa highlight that many taxa (e.g., *Actinomarinales, Marine Group II, Marinimicrobia (SAR406 clade), Nitrosopumilales, Parvibaculales, SAR11 clade*, *Flavobacteriales, Puniceispirillales, Rhodobacterales, Rhodospirillales, Synechococcales, Bacillariophyta*, *Chlorellales, Mamiellales, Parmales,* and *Phaeocystales*) deviate from the 1:1 RNA:DNA line. If microbes were passively being transported along the salinity gradient, relative abundance and putatively active microbes would scale proportionally (Chícharo & Chícharo, 2008). In contrast we observe that many orders do follow that trend (Figure 5), suggesting microbial orders are either more abundant than active, or active than abundant (Chícharo & Chícharo, 2008). These large discrepancies suggest active reorganization of the microbial community along this salinity gradient as they respond to changing nutrient and OM signatures and increased salinity (Sipler et al., 2017; Tee et al., 2021; Zeglin, 2015). These results exhibit and support that microbial community composition can significantly change, even across fine spatial scales at river-ocean interfaces (Anderson & Harvey, 2022).

The identified environmental drivers of putatively active microbial taxa (Figure 6) were salinity, POC and SiO_2 concentrations, and condensed aromatic and aromatic compounds. Many of these variables themselves reflect increasing

salinity, and ongoing transformation of organic matter (Figure 6; Table A9). Condensed aromatic and aromatic compounds are key indicators of shifts from allochthonous to autochthonous organic matter sources, tightly linked to salinity gradients (Mook, 2000; Murphy et al., 2008; Sleighter & Hatcher, 2008; Yu et al., 2010). In contrast, POC and SiO_2 likely largely reflect increasing primary production, particularly for *Bacillariophyta*, a key marine diatom who utilizes SiO_2 for building frustules for its cells (Q. Chen et al., 2025; Dagg et al., 2004; Di Grazia et al., 2023; Yool & Tyrrell, 2003).

Well established river to ocean biogeochemical gradients realized over small spatial scales

Coupled with the existence of clear spatial trends in nutrient and carbon and microbial community dynamics, several biogeochemical trends were visible within these small rain-dominated river plumes at unprecedented scales. Stable isotope signatures for carbon and nitrogen are key indicators of allochthonous and autochthonous sources with typical signatures increasing from freshwaters to oceans with a shift from allochthonous (terrestrial-derived matter) to autochthonous (phytoplankton growth and microbial production derived matter) (Sleighter & Hatcher, 2008). δ^{13}C-DOC and δ^{13}C-POC in particular are well established tracers of terrestrial and marine materials in the NPCTR (St. Pierre et al., 2020). Our results show significant increases in stable isotope signatures (δ^{15}N-PN , δ^{13}C-DOC & δ^{13}C-POC), consistent with these established trends (Mook, 2000; Murphy et al., 2008; Yu et al., 2010). DOM compound classes exhibited decreases in condensed aromatic and aromatic compounds consistent with shifting contributions of terrestrial vs marine sources. CHON and C/N ratios are common parameters for establishing contribution of nitrogen to environmental samples (Z. L. Chen et al., 2023; Maranger et al., 2018). Given increases in CHON signatures and decreasing C/N ratios, these results suggest an enrichment of nitrogen within the water column with distance from the creek mouth (i.e., marine DOM is enhanced with nitrogen), aligning with existing literature (Hawkes et al., 2020; Maranger et al., 2018; Ren et al., 2024; Sleighter & Hatcher, 2008).

Terrestrial DOM (i.e., freshwater exports) is typically enriched in more complex, aromatic, and less labile compounds, shifting towards a more labile, aliphatic, and protein-rich microbially processed DOM seaward (Z. L. Chen et al., 2023; Leyva et al., 2022; Medeiros et al., 2016; Mori et al., 2019). Our study reflects these findings, which, in theory, should lead to preferential degradation of organic matter in freshwaters and primary production in marine ecosystems (Wu et al., 2018). In practice, we note that this is not entirely the case, while terrestrial DOM is relatively more aromatic, aliphatic compounds spike around site 1 and 2 (79 and 279 m from the creek mouth), then rapidly decrease (Figure 4). At this distance, we note a mirrored rapid enrichment and then depletion in relative abundance of *Burkholderiales* (Figure 5), highlighting a potential key hotspot of preferential aromatic reprocessing by *Burkholderiales*, an order recognized for efficient aromatic degradation (Pérez-Pantoja et al., 2012), and further aligning with a potential transition area of the river plume (Figure 3). This demonstrates that these thin

freshwater surfaces are not static, with shifting chemical and potential biological hotspots/hot moments along salinity gradients (McClain et al., 2003).

Ultimately, changes in biogeochemical signatures with increasing depth and distance from the creek mouth align with many of the primary gradients and trends within existing peer-reviewed land-ocean literature, the key difference being the scale of the ecosystem connections (Hunt et al., 2024; Maranger et al., 2018; Sleighter & Hatcher, 2008; St. Pierre et al., 2021). Many of the observed trends (i.e. non-conservative mixing, dilution of inorganic nutrients, shift from phosphorous to nitrogen limitation, increases in the carbon and nitrogen stable isotope signatures and nitrogen containing DOM signatures, loss of aromaticity, and the ubiquitous nature of hotspots and hot moments) are realized over scales of 15 cm or less, which is, to the best of our knowledge, considerably higher resolution than previously investigated (Giesbrecht et al., 2025a; Hunt et al., 2024; St. Pierre et al., 2021). The persistence of these gradients suggests that key processes observed in larger freshwater-ocean plumes are also visible within small rain-dominated river plumes at much finer spatial scales, emphasizing the need to refine sampling techniques to resolve this gap.

Broader NPCTR implications, limitations, and future directions

Though the Hyacinthe Creek estuary is only one of thousands of small, rain-dominated river plumes within the NPCTR, the spatial scales and integration of a holistic catalogue of biogeochemical variables in this study sheds light for the first time on how microbial and nutrient regimes shift within these shallow small river plumes. We recognize that river-ocean plumes are highly dynamic, which constrains the extent to which these results can be extrapolated to other seasonal or climatic conditions and systems beyond our study. Although winter (December to February) in the NPCTR is characterized by large rainfall events, therefore recognized as the period of highest freshwater influence (St. Pierre et al. 2020), an extended period of clear, calm, and dry conditions around the time of sampling (Figure A1), dampened the freshwater influence and resulted in an early spring bloom (NASA Worldview, 2022).

Ultimately, this sampling was conducted on only one of the 14 NPCTR watershed types: the rain hills-central (RHC) watershed type (Giesbrecht et al., 2022, 2025a). The RHC is located from central British Columbia to Washington, defined by a rain-dominated climate with moderate precipitation (MAP ~ 2720 mm) and high evapotranspiration relative to other coastal watersheds (Giesbrecht et al., 2022, 2025a). Given its rain-dominated climate, moderate to high DOM, lower inorganic nutrient concentrations, and hilly terrain, it shares similar characteristics to the rain hills-northern (RHN) and rain lowlands central (RLC) watershed types of the NPCTR. Distinctions between the focal RHC watershed type and RHN and RLC include precipitation (RHC < RHN), evapotranspiration (RHC > RHN), pH and alkalinity (RHC > RLC), SiO_2 concentrations (RHC > RLC) and terrain (RHC > RLC) (Giesbrecht et al., 2022, 2025a). Though rain-dominated watershed types have some

similarities, these fundamental differences highlight the need for similar fine-scaled approaches to be conducted throughout the year and across the diversity of watershed types within the NPCTR region.

This study clearly demonstrates that the established biogeochemical and microbial trends of aromaticity shifts, inorganic nutrient dilution, hotspot persistence, and microbial river-to-sea continuum exists even over extremely small scales in small rain-dominated river plumes, a vertical resolution often overlooked in traditional oceanography (Aoki et al., 2022; Sahoo et al., 2025). These findings raise questions about the representation of surface layer processes along coastlines and highlights the need for integrative approaches of characterizing small river plumes. Conceptually, this advances our current understanding and frameworks within not only the NPCTR (Giesbrecht et al., 2022, 2025) but small river plumes globally. Though variable in freshwater discharge, geography, geomorphology, dilution rates, vertical mixing, and transport (Horner-Devine et al., 2015), small river plumes likely share a common feature: a thin surface lens that mediates transformations in microbial and biogeochemical signatures. Recognizing and characterizing these miniature plumes create new avenues for improving our understanding of small river plumes in coastal zones at land-ocean interfaces.

Summary and Implications

Previous work in coastal waters globally has demonstrated consistent, reoccurring patterns in organic carbon, nutrient, and microbial community composition across coastal waters. Whereas this work focused on coastal waters affected by large rivers, the plumes of which can extend multiple meters in depth and kilometers in extent, here we show that these same biogeochemical gradients occur across small rain-dominated river plumes over scales of 15 centimeters or less. We also identify significant heterogeneity across these small river plumes, such that these hotspots or hot moments play potentially important roles in the reprocessing of terrestrial materials. This study provides a basis for understanding small rain-dominated river plumes and opens the door for the development of interdisciplinary frameworks for studying highly dynamic freshwater-ocean interfaces globally.

Acknowledgements

We acknowledge that this research was conducted within the Traditional Territories of Indigenous Nations including the Wei Wai Kai, Wei Wai Kum, Homalco, Klahoose, and K'omoks First Nations who have maintained a deep and ongoing relationship with these lands and waters since time immemorial. We express gratitude to the Ján Veizer Stable Isotope Laboratory, UC Davis Stable Isotope Laboratory, and the University of Alberta Biogeochemical Analytical Service Laboratory that contributed to the analysis of this study's data. Additionally, we extend our appreciation to Natalie Benoit from the University of British Columbia and Emily Haughton from the Hakai Institute for their guidance and support throughout this project. The research was supported by the Tula Foundation.

References

Anderson, N. J., Heathcote, A. J., Engstrom, D. R., Ryves, D. B., Mills, K., Prairie, Y. T., del Giorgio, P. A., Bennion, H., Turner, S., Rose, N. L., Jones, V. J., Solovieva, N., Cook Shinneman, A., Umbanhowar, C. E., Fritz, S. C., Verschuren, D., Saros, J. E., Russell, J. M., Bindler, R., … Myrbo, A. E. (2020). Anthropogenic alteration of nutrient supply increases the global freshwater carbon sink. *Science Advances*, *6*(16). https://doi.org/10.1126/sciadv.aaw2145

Anderson, S. R., & Harvey, E. L. (2022). Estuarine microbial networks and relationships vary between environmentally distinct communities. *PeerJ*, *10*, e14005. https://doi.org/10.7717/PEERJ.14005/SUPP-11

Aoki, L. R., Brisbin, M. M., Hounshell, A. G., Kincaid, D. W., Larson, E. I., Sansom, B. J., Shogren, A. J., Smith, R. S., & Sullivan-Stack, J. (2022). Preparing Aquatic Research for an Extreme Future: Call for Improved Definitions and Responsive, Multidisciplinary Approaches. *Bioscience*, *72*(6), 508. https://doi.org/10.1093/BIOSCI/BIAC020

Baker, G. C., Smith, J. J., & Cowan, D. A. (2003). Review and re-analysis of domain-specific 16S primers. *Journal of Microbiological Methods*, *55*(3), 541–555. https://doi.org/10.1016/j.mimet.2003.08.009

Basdurak, N. B., Largier, J. L., & Nidzieko, N. J. (2020). Modeling the Dynamics of Small-Scale River and Creek Plumes in Tidal Waters. *Journal of Geophysical Research: Oceans*, *125*(7), e2019JC015737. https://doi.org/10.1029/2019JC015737

Benitez-Nelson, C. R. (2000). The biogeochemical cycling of phosphorus in marine systems. *Earth-Science Reviews*, *51*(1–4), 109–135. https://doi.org/10.1016/S0012-8252(00)00018-0

Bernard, C. Y., D ¨ Urr, H. H., Heinze, C., Segschneider, J., & Maier-Reimer, E. (2011). Contribution of riverine nutrients to the silicon biogeochemistry of the global ocean-a model study. *Biogeosciences*, *8*, 551–564. https://doi.org/10.5194/bg-8-551-2011

Bertin, C., Carroll, D., Menemenlis, D., Dutkiewicz, S., Zhang, H., Schwab, M., Savelli, R., Matsuoka, A., Manizza, M., Miller, C. E., Bowring, S., Guenet, B., & Le Fouest, V. (2025). Paving the Way for Improved Representation of Coupled Physical and Biogeochemical Processes in Arctic River Plumes—A Case Study of the Mackenzie Shelf. *Permafrost and Periglacial Processes*. https://doi.org/10.1002/ppp.2271

Bianchi, T. S., Allison, M. A., & Cai, W.-J. (2014). *Biogeochemical dynamics at major river-coastal interfaces : linkages with global change*. 658.

Bianchi, T. S., Arndt, S., Austin, W. E. N., Benn, D. I., Bertrand, S., Cui, X., Faust, J. C., Koziorowska-Makuch, K., Moy, C. M., Savage, C., Smeaton, C., Smith, R. W., & Syvitski, J. (2020). Fjords as Aquatic Critical Zones (ACZs). *Earth-Science Reviews*, *203*, 103145. https://doi.org/10.1016/J.EARSCIREV.2020.103145

Bidlack, A. L., Bisbing, S. M., Buma, B. J., Fellman, J. B., Floyd, W. C., Giesbrecht, I., Lally, A., Lertzman, K. P., Perakis, S. S., Butman, D. E., D'amore, D. V., Fleming, S. W., Hood, E. W., Hunt, B. P. V., Kiffney, P. M., Mcnicol, G., Menounos, B., & Tank, S. E. (2021). Climate-Mediated Changes to Linked Terrestrial and Marine Ecosystems across the Northeast Pacific Coastal Temperate Rainforest Margin. *BioScience*, *71*(6), 581–595. https://doi.org/10.1093/biosci/biaa171

Bokulich, N. A., Kaehler, B. D., Rideout, J. R., Dillon, M., Bolyen, E., Knight, R., Huttley, G. A., & Gregory Caporaso, J. (2018). Optimizing taxonomic classification of marker-gene amplicon sequences with QIIME 2's q2-feature-classifier plugin. *Microbiome*, *6*(1). https://doi.org/10.1186/s40168-018-0470-z

Borcard, D., Gillet, F., & Legendre, P. (2011). Numerical Ecology with R. *Numerical Ecology with R*. https://doi.org/10.1007/978-1-4419-7976-6

Buttigieg, P. L., & Ramette, A. (2014). A guide to statistical analysis in microbial ecology: A community-focused, living review of multivariate data analyses. *FEMS Microbiology Ecology*, *90*(3), 543–550. https://doi.org/10.1111/1574-6941.12437

Campitelli, E. (2025). ggnewscale: Multiple Fill and Colour Scales in "ggplot2" [R package ggnewscale version 0.5.2]. *CRAN: Contributed Packages*. https://doi.org/10.32614/CRAN.package.ggnewscale

Carmack, E., Winsor, P., & Williams, W. (2015). The contiguous panarctic Riverine Coastal Domain: A unifying concept. *Progress in Oceanography*, *139*, 13–23. https://doi.org/10.1016/J.POCEAN.2015.07.014

CCN. (2022). *Daily Data Report for 2022*. https://climate.weather.gc.ca/climate_data/daily_data_e.html?hlyRange=%7C&dlyRange=1984-04-01%7C2022-12-30&mlyRange=1984-01-01%7C2007-02-01&climate_id=1023462&Prov=BC&urlExtension=_e.html&searchType=stnName&optLimit=yearRange&StartYear=2022&EndYear=2023&selRowPerPage=25&Line=0&searchMethod=contains&Month=12&Day=14&txtStationName=heriot+bay+se&timeframe=2&Year=2022

Chen, F., & MacDonald, D. G. (2006). Role of mixing in the structure and evolution of a buoyant discharge plume. *Journal of Geophysical Research: Oceans*, *111*(11), 11002. https://doi.org/10.1029/2006JC003563

Chen, Q., Li, Y., Chen, C. T. A., Jiang, Z. P., Cai, W. J., Pan, H., Shen, Y., Ding, Z., Di, Y., Zhu, C., Jiao, N., & Pan, Y. (2025). Diatom-induced calcification in coastal marine environments: Biomineralization threshold and mechanism. *Marine Chemistry*, *271*, 104533. https://doi.org/10.1016/j.marchem.2025.104533

Chen, Z. L., Yi, Y., Zhang, H., Li, P., Wang, Y., Yan, Z., Wang, K., He, C., Shi, Q., & He, D. (2023). Differences in Dissolved Organic Matter Molecular Composition along Two Plume Trajectories from the Yangtze River Estuary to the East China Sea. *ACS Environmental Au*, *4*(1), 31. https://doi.org/10.1021/ACSENVIRONAU.3C00030

Chícharo, M. A., & Chícharo, L. (2008). RNA:DNA Ratio and Other Nucleic Acid Derived Indices in Marine Ecology. *International Journal of Molecular Sciences*, *9*(8), 1453. https://doi.org/10.3390/ijms9081453

Chuvochina, M., Gerken, J., Frentrup, M., Sandikci, Y., Goldmann, R., Freese, H. M., Göker, M., Sikorski, J., Yarza, P., Quast, C., Peplies, J., Glöckner, F. O., & Reimer, L. C. (2026). SILVA in 2026: a global core biodata resource for rRNA within the DSMZ digital diversity. *Nucleic Acids Research*, *54*(D1), D334–D341. https://doi.org/10.1093/nar/gkaf1247

Correll, D. L. (1999). Phosphorus: a rate limiting nutrient in surface waters. *Poultry Science*, *78*(5), 674–682. https://doi.org/10.1093/ps/78.5.674

Costanza, R., d'Arge, R., de Groot, R., Farber, S., Grasso, M., Hannon, B., Limburg, K., Naeem, S., O'Neill, R. V., Paruelo, J., Raskin, R. G., Sutton, P., & van den Belt, M. (1998). The value of the world's ecosystem services and natural capital. *Ecological Economics*, *25*(1), 3–15. https://doi.org/10.1016/s0921-8009(98)00020-2

da Cunha, L. C. (2020). *Coastal Nutrient Supply and Global Ocean Biogeochemistry*. https://doi.org/10.1007/978-3-319-71064-8_115-1

Dagg, M., Benner, R., Lohrenz, S., & Lawrence, D. (2004). Transformation of dissolved and particulate materials on continental shelves influenced by large rivers: Plume processes. *Continental Shelf Research*, *24*(7–8), 833–858. https://doi.org/10.1016/j.csr.2004.02.003

DellaSala, D. A. (2011). Temperate and Boreal Rainforests of the World: Ecology and Conservation. *Temperate and Boreal Rainforests of the World: Ecology and Conservation*. https://doi.org/10.5822/978-1-61091-008-8

Di Grazia, F., Garcia, X., Acuña, V., Llanos-Paez, O., Galgani, L., Gumiero, B., & Loiselle, S. A. (2023). Modeling dissolved and particulate organic carbon dynamics at basin and sub-basin scales. *Science of The Total Environment*, *884*(G1), 163840. https://doi.org/10.1016/j.scitotenv.2023.163840

Discovery Islands Forest Conservation Project. (2022, May 14). *Hyacinthe Creek Watershed*. https://www.discoveryislandsforestconservationproject.ca/watersheds-of-quadra-island/8/

Dray S, Bauman D, Blanchet G, Borcard D, Clappe S, Guénard G, Jombart T, Larocque G, Legendre P, Madi N, & Wagner HH. (2025). adespatial: Multivariate Multiscale Spatial Analysis. . *R Package*, *0.3-28*. https://doi.org/10.18637/jss.v103.i07

ESRI. (2009). *World Imagery Basemap* (Last updated: March 3, 2026). ESRI. https://www.arcgis.com/home/item.html?id=10df2279f9684e4a9f6a7f08febac2a9

ESRI. (2025a). *ArcGIS Pro [Software]* (3.6). Esri.

ESRI. (2025b). Empirical Bayesian Kriging 3D (Geostatistical Analyst). In *ArcGIS Pro* (3.6). ArcGIS Pro. https://pro.arcgis.com/en/pro-app/latest/tool-reference/geostatistical-analyst/empirical-bayesian-kriging-3d.htm

ESRI. (2025c). *GA Layer 3D To NetCDF (Geostatistical Analyst)* (3.6). ArcGIS Pro. https://pro.arcgis.com/en/pro-app/latest/tool-reference/geostatistical-analyst/ga-layer-3d-to-netcdf.htm

ESRI, DeLorme, HERE, & MapmyIndia. (2011). *World Light Gray Base*. Esri. https://www.arcgis.com/home/item.html?id=ed712cb1db3e4bae9e85329040fb9a49

Fry, B. (2002). Conservative mixing of stable isotopes across estuarine salinity gradients: A conceptual framework for monitoring watershed influences on downstream fisheries production. *Estuaries*, *25*(2), 264–271. https://doi.org/10.1007/BF02691313/METRICS

Gardner, A. S., Moholdt, G., Cogley, J. G., Wouters, B., Arendt, A. A., Wahr, J., Berthier, E., Hock, R., Pfeffer, W. T., Kaser, G., Ligtenberg, S. R. M., Bolch, T., Sharp, M. J., Hagen, J. O., Van Den Broeke, M. R., & Paul, F. (2013). A reconciled estimate of glacier contributions to sea level rise: 2003 to 2009. *Science*, *340*(6134), 852–857. https://doi.org/10.1126/science.1234532

Geyer, W. R. (2010). Estuarine salinity structure and circulation. *Contemporary Issues in Estuarine Physics*, 12–26. https://doi.org/10.1017/CBO9780511676567.003

Giesbrecht, I. J. W., Lertzman, K. P., Tank, S. E., Frazer, G. W., St. Pierre, K. A., Gonzalez Arriola, S., Desmarais, I., & Haughton, E. (2025a). Mapping the Spatial Heterogeneity of Watershed Ecosystems and Water Quality in Rainforest Fjordlands. *Ecosystems 2025 28:2*, *28*(2), 1–29. https://doi.org/10.1007/S10021-025-00964-X

Giesbrecht, I. J. W., Lertzman, K. P., Tank, S. E., Frazer, G. W., St. Pierre, K. A., Gonzalez Arriola, S., Desmarais, I., & Haughton, E. (2025b, February 13). *Dryad | Data: Mapping the spatial heterogeneity of watershed ecosystems and water quality in rainforest fjordlands*. DRYAD. https://datadryad.org/dataset/doi:10.5061/dryad.qv9s4mwp6

Giesbrecht, I. J. W., Tank, S. E., Frazer, G. W., Hood, E., Gonzalez Arriola, S. G., Butman, D. E., D'Amore, D. V., Hutchinson, D., Bidlack, A., & Lertzman, K. P. (2022). Watershed Classification Predicts Streamflow Regime and Organic Carbon Dynamics in the Northeast Pacific Coastal Temperate Rainforest. *Global Biogeochemical Cycles*, *36*(2). https://doi.org/10.1029/2021GB007047

Gobler, C. J. (2020). Climate Change and Harmful Algal Blooms: Insights and perspective. *Harmful Algae*, *91*, 101731. https://doi.org/10.1016/J.HAL.2019.101731

Gonzalez Arriola, S., Giesbrecht, I. J. W., Biles, F. E., & D'Amore, D. V. (2018). *Watersheds of the northern Pacific coastal temperate rainforest margin [Data set]*. Hakai Institute. https://doi.org/10.21966/1.715755

Guillou, L., Bachar, D., Audic, S., Bass, D., Berney, C., Bittner, L., Boutte, C., Burgaud, G., De Vargas, C., Decelle, J., Del Campo, J., Dolan, J. R., Dunthorn, M., Edvardsen, B., Holzmann, M., Kooistra, W. H. C. F., Lara, E., Le Bescot, N., Logares, R., … Christen, R. (2013). The Protist Ribosomal Reference database (PR2): a catalog of unicellular eukaryote Small Sub-Unit rRNA sequences with curated taxonomy. *Nucleic Acids Research*, *41*(D1), D597–D604. https://doi.org/10.1093/nar/gks1160

Haas, S., Robicheau, B. M., Rakshit, S., Tolman, J., Algar, C. K., LaRoche, J., & Wallace, D. W. R. (2021). Physical mixing in coastal waters controls and decouples nitrification via biomass dilution. *Proceedings of the National Academy of Sciences of the United States of America*, *118*(18), e2004877118. https://doi.org/10.1073/pnas.2004877118

Harris, G. P. (1986). The concept of limiting nutrients. *Phytoplankton Ecology*, 137–165. https://doi.org/10.1007/978-94-009-3165-7_7

Hawkes, J. A., D'Andrilli, J., Agar, J. N., Barrow, M. P., Berg, S. M., Catalán, N., Chen, H., Chu, R. K., Cole, R. B., Dittmar, T., Gavard, R., Gleixner, G., Hatcher, P. G., He, C., Hess, N. J., Hutchins, R. H. S., Ijaz, A., Jones, H. E., Kew, W., … Podgorski, D. C. (2020). An international laboratory comparison of dissolved organic matter composition by high resolution mass spectrometry: Are we getting the same answer? *Limnology and Oceanography: Methods*, *18*(6), 235–258. https://doi.org/10.1002/lom3.10364

Herbert, R. A. (1999). Nitrogen cycling in coastal marine ecosystems. *FEMS Microbiology Reviews*, *23*(5), 563–590. https://doi.org/10.1111/J.1574-6976.1999.TB00414.X

Horner-Devine, A. R., Hetland, R. D., & MacDonald, D. G. (2015). Mixing and transport in coastal river plumes. *Annual Review of Fluid Mechanics*, *47*(Volume 47, 2015), 569–594. https://doi.org/10.1146/ANNUREV-FLUID-010313-141408/CITE/REFWORKS

Howard, M. D. A., Smith, J., Caron, D. A., Kudela, R. M., Loftin, K., Hayashi, K., Fadness, R., Fricke, S., Kann, J., Roethler, M., Tatters, A., & Theroux, S. (2022). Integrative monitoring strategy for marine and freshwater harmful algal blooms and toxins across the freshwater-to-marine continuum. *Integrated Environmental Assessment and Management*, *19*(3), 586. https://doi.org/10.1002/IEAM.4651

Howarth, R. W., & Marino, R. (2006). Nitrogen as the limiting nutrient for eutrophication in coastal marine ecosystems: Evolving views over three decades. *Limnology and Oceanography*, *51*(1 II). https://doi.org/10.4319/lo.2006.51.1_part_2.0364

Hugerth, L. W., & Andersson, A. F. (2017). Analysing microbial community composition through amplicon sequencing: From sampling to hypothesis testing. *Frontiers in Microbiology*, *8*(SEP), 274218. https://doi.org/10.3389/fmicb.2017.01561

Hunt, B. P. V., Alin, S., Bidlack, A., Diefenderfer, H. L., Jackson, J. M., Kellogg, C. T. E., Kiffney, P., St. Pierre, K. A., Carmack, E., Floyd, W. C., Hood, E., Horner-Devine, A. R., Levings, C., & Vargas, C. A. (2024). Advancing an integrated understanding of land–ocean connections in shaping the marine ecosystems of coastal temperate rainforest ecoregions. In *Limnology and Oceanography* (Vol. 69, Number 12, pp. 3061–3096). John Wiley and Sons Inc. https://doi.org/10.1002/lno.12724

Hutchins, R. H. S., Aukes, P., Schiff, S. L., Dittmar, T., Prairie, Y. T., & del Giorgio, P. A. (2017). The Optical, Chemical, and Molecular Dissolved Organic Matter Succession Along a Boreal Soil-Stream-River Continuum. *Journal of Geophysical Research: Biogeosciences*, *122*(11), 2892–2908. https://doi.org/10.1002/2017JG004094

James, W. F., Sorge, P. W., & Garrison, P. J. (2015). Managing internal phosphorus loading and vertical entrainment in a weakly stratified eutrophic lake. *Lake and Reservoir Management*, *31*(4), 292–305. https://doi.org/10.1080/10402381.2015.1079755

Jari Oksanen, Gavin L. Simpson, F. Guillaume Blanchet, Roeland Kindt, Pierre Legendre, Peter R. Minchin, R.B. O'Hara, Peter Solymos, M. Henry H. Stevens, Eduard Szoecs, Helene Wagner, Matt Barbour, Michael Bedward, Ben Bolker, Daniel Borcard, Tuomas Borman, Gustavo Carvalho, Michael Chirico, Miquel De Caceres, … James Weedon. (2025). *Package "vegan": Community Ecology Package*. *2.7-2*. https://github.com/vegandevs/vegan

Jiao, N., Robinson, C., Azam, F., Thomas, H., Baltar, F., Dang, H., Hardman-Mountford, N. J., Johnson, M., Kirchman, D. L., Koch, B. P., Legendre, L., Li, C., Liu, J., Luo, T., Luo, Y. W., Mitra, A., Romanou, A., Tang, K., Wang, X., … Zhang, R. (2014). Mechanisms of microbial carbon sequestration in the ocean - Future research directions. *Biogeosciences*, *11*(19), 5285–5306. https://doi.org/10.5194/bg-11-5285-2014

Kellogg, C. (2024). *Seawater Filtration for Microbial or Environmental DNA v1*. https://doi.org/10.17504/PROTOCOLS.IO.RM7VZJXRRLX1/V1

Kellogg, C., Carvalho, rute. carvalho, Prentice, C., & Robinson, K. (2024). *Preparing multiplexed 16S rRNA gene amplicons (with fusion primers) for the Illumina MiSeq v1*. https://doi.org/10.17504/protocols.io.3byl49842go5/v1

Kim, B. K., Jeon, M., Joo, H. M., Kim, T. W., Park, S. J., Park, J., & Ha, S. Y. (2021). Impact of Freshwater Discharge on the Carbon Uptake Rate of Phytoplankton During Summer (January–February 2019) in Marian Cove, King George Island, Antarctica. *Frontiers in Marine Science*, *8*, 725173. https://doi.org/10.3389/FMARS.2021.725173/BIBTEX

Koch, B. P., & Dittmar, T. (2006). From mass to structure: An aromaticity index for high-resolution mass data of natural organic matter. *Rapid Communications in Mass Spectrometry*, *20*(5), 926–932. https://doi.org/10.1002/rcm.2386

Krause, J. W., Duarte, C. M., Marquez, I. A., Assmy, P., Fernández-Méndez, M., Wiedmann, I., Wassmann, P., Kristiansen, S., & Agustí, S. (2018). Biogenic silica production and diatom dynamics in the Svalbard region during spring. *Biogeosciences*, *15*(21), 6503–6517. https://doi.org/10.5194/bg-15-6503-2018

Legendre, P., & Gallagher, E. D. (2001). Ecologically meaningful transformations for ordination of species data. *Oecologia*, *129*(2), 271–280. https://doi.org/10.1007/S004420100716

Leyva, D., Jaffé, R., Courson, J., Kominoski, J. S., Tariq, M. U., Saeed, F., & Fernandez-Lima, F. (2022). Molecular level characterization of DOM along a freshwater-to-estuarine coastal gradient in the Florida Everglades. *Aquatic Sciences*, *84*(4), 63. https://doi.org/10.1007/S00027-022-00887-Y

Loder, T. C., & Reichard, R. P. (1981). The dynamics of conservative mixing in estuaries. *Estuaries*, *4*(1), 64–69. https://doi.org/10.2307/1351543

Loreau, M., Mouquet, N., & Holt, R. D. (2003). Meta-ecosystems: A theoretical framework for a spatial ecosystem ecology. *Ecology Letters*, *6*(8), 673–679. https://doi.org/10.1046/J.1461-0248.2003.00483.X

Madsen, E. L. (2008). *Environmental microbiology From genomes to biochemistry*. 467.

Maranger, R., Jones, S. E., & Cotner, J. B. (2018). Stoichiometry of carbon, nitrogen, and phosphorus through the freshwater pipe. *Limnology And Oceanography Letters*, *3*(3), 89–101. https://doi.org/10.1002/LOL2.10080

Martínez, M. L., Intralawan, A., Vázquez, G., Pérez-Maqueo, O., Sutton, P., & Landgrave, R. (2007). The coasts of our world: Ecological, economic and social importance. *Ecological Economics*, *63*(2–3), 254–272. https://doi.org/10.1016/j.ecolecon.2006.10.022

McClain, M. E., Boyer, E. W., Dent, C. L., Gergel, S. E., Grimm, N. B., Groffman, P. M., Hart, S. C., Harvey, J. W., Johnston, C. A., Mayorga, E., McDowell, W. H., & Pinay, G. (2003). Biogeochemical Hot Spots and Hot Moments at the Interface of Terrestrial and Aquatic Ecosystems. *Ecosystems*, *6*(4), 301–312. https://doi.org/10.1007/s10021-003-0161-9

McNichol, J., Williams, N. L. R., Raut, Y., Carlson, C., Halewood, E. R., Turk-Kubo, K., Zehr, J. P., Rees, A. P., Tarran, G., Gradoville, M. R., Wietz, M., Bienhold, C., Metfies, K., Torres-Valdés, S., Mock, T., Eggers, S. L., Jeffrey, W., Moss, J., Berube, P., … Fuhrman, J. (2025). Characterizing organisms from three domains of life with universal primers from throughout the global ocean. *Scientific Data 2025 12:1*, *12*(1), 1078-. https://doi.org/10.1038/s41597-025-05423-9

McNicol, G., Bulmer, C., D'Amore, D., Sanborn, P., Saunders, S., Giesbrecht, I., Arriola, S. G., Bidlack, A., Butman, D., & Buma, B. (2019). Large, climate-sensitive soil carbon stocks mapped with pedology-informed machine learning in the North Pacific coastal temperate rainforest. *Environmental Research Letters*, *14*(1), 014004. https://doi.org/10.1088/1748-9326/aaed52

McNicol, G., Hood, E., Butman, D. E., Tank, S. E., Giesbrecht, I. J. W., Floyd, W., D'Amore, D., Fellman, J. B., Cebulski, A., Lally, A., McSorley, H., & Gonzalez Arriola, S. G. (2023). Small, Coastal Temperate Rainforest Watersheds Dominate Dissolved Organic Carbon Transport to the Northeast Pacific Ocean. *Geophysical Research Letters*, *50*(12), e2023GL103024. https://doi.org/10.1029/2023GL103024

Medeiros, P. M., Seidel, M., Niggemann, J., Spencer, R. G. M., Hernes, P. J., Yager, P. L., Miller, W. L., Dittmar, T., & Hansell, D. A. (2016). A novel molecular approach for tracing terrigenous dissolved organic matter into the deep ocean. *Global Biogeochemical Cycles*, *30*(5), 689–699. https://doi.org/10.1002/2015GB005320

Menge, B. A., Caselle, J. E., Milligan, K., Gravem, S. A., Gouhier, T. C., White, J. W., Barth, J. A., Blanchette, C. A., Carr, M. H., Chan, F., Lubchenco, J., McManus, M. A., Novak, M., Raimondi, P. T., & Washburn, L. (2019). Integrating coastal oceanic and benthic ecological approaches for understanding large-scale meta-ecosystem dynamics. *Oceanography*, *32*(3), 38–49. https://doi.org/10.5670/OCEANOG.2019.309

Mook, W. G. (2000). Environmental Isotopes in the Hydrological Cycle : Principles and Applications Volume I. *International Hydrological Programme*, *1*.

Moore, C. M., Mills, M. M., Arrigo, K. R., Berman-Frank, I., Bopp, L., Boyd, P. W., Galbraith, E. D., Geider, R. J., Guieu, C., Jaccard, S. L., Jickells, T. D., La Roche, J., Lenton, T. M., Mahowald, N. M., Marañón, E., Marinov, I., Moore, J. K., Nakatsuka, T., Oschlies, A., … Ulloa, O. (2013). Processes and patterns of oceanic nutrient limitation. In *Nature Geoscience* (Vol. 6, Number 9, pp. 701–710). https://doi.org/10.1038/ngeo1765

Mori, C., Santos, I. R., Brumsack, H. J., Schnetger, B., Dittmar, T., & Seidel, M. (2019). Non-conservative behavior of dissolved organic matter and trace metals (Mn, Fe, Ba) driven by porewater exchange in a subtropical mangrove-estuary. *Frontiers in Marine Science*, *6*(JUL), 465666. https://doi.org/10.3389/FMARS.2019.00481/BIBTEX

Murphy, K. R., Stedmon, C. A., Waite, T. D., & Ruiz, G. M. (2008). Distinguishing between terrestrial and autochthonous organic matter sources in marine environments using fluorescence spectroscopy. *Marine Chemistry*, *108*(1–2), 40–58. https://doi.org/10.1016/j.marchem.2007.10.003

NASA Worldview. (2022). NASA Worldview. In *NASA Worldview*. MODIS / NASA Earth Observatory. https://worldview.earthdata.nasa.gov/?v=-128.35677400209124,48.74207111837932,-121.79941944665767,51.85339924337932&l=Reference_Labels_15m(hidden),Reference_Features_15m(hidden),Coastlines_15m,S3B_OLCI_Chlorophyll_a,S3A_OLCI_Chlorophyll_a(hidden)&lg=false&t=2026-03-15-T14%3A54%3A51Z

Ngatia, L., Grace III, J. M., Moriasi, D., & Taylor, R. (2019). *Nitrogen and Phosphorus Eutrophication in Marine Ecosystems*. https://doi.org/10.5772/intechopen.81869

O'Donnell, J., Ackleson, S. G., & Levine, E. R. (2008). On the spatial scales of a river plume. *Journal of Geophysical Research: Oceans*, *113*(4). https://doi.org/10.1029/2007JC004440

Oliver, A. A., Tank, S. E., Giesbrecht, I., Korver, M. C., Floyd, W. C., Sanborn, P., Bulmer, C., & Lertzman, K. P. (2017). A global hotspot for dissolved organic carbon in hypermaritime watersheds of coastal British Columbia. *BIOGEOSCIENCES*, *14*(15), 3743–3762. https://doi.org/10.5194/bg-14-3743-2017

OpenAI. (2025). ChatGPT. In *GPT-5.2* (GPT-5.2). https://chat.openai.com/

Orlova, J., Amiri, F., Bourgeois, A. K., Buttle, J. M., Cherlet, E., Cuss, C. W., Devito, K. J., Emelko, M. B., Floyd, W. C., Foster, D. E., Hutchins, R. H. S., Jamieson, R., Johnson, M. S., McSorley, H. J., Silins, U., Tank, S. E., Thompson, L. M., Webster, K. L., Williams, C. H. S., & Olefeldt, D. (2024). Composition of Stream Dissolved Organic Matter Across Canadian Forested Ecozones Varies in Three Dimensions Linked to Landscape and Climate. *Water Resources Research*, *60*(5). https://doi.org/10.1029/2023WR035196

Paliy, O., & Shankar, V. (2016). Application of multivariate statistical techniques in microbial ecology. *Molecular Ecology*, *25*(5), 1032. https://doi.org/10.1111/MEC.13536

Pedersen, T. L. (2025). ggforce: Accelerating "ggplot2" [R package ggforce version 0.5.0]. *CRAN: Contributed Packages*. https://doi.org/10.32614/CRAN.package.ggforce

Pérez-Pantoja, D., Donoso, R., Agulló, L., Córdova, M., Seeger, M., Pieper, D. H., & González, B. (2012). Genomic analysis of the potential for aromatic compounds biodegradation in Burkholderiales. *Environmental Microbiology*, *14*(5), 1091–1117. https://doi.org/10.1111/J.1462-2920.2011.02613.X;WEBSITE:WEBSITE:SFAMJOURNALS;WGROUP:STRING:PUBLICATION

Plont, S., Scott, D. T., & Hotchkiss, E. R. (2023). Biogeochemical Processes Are Altered by Non-Conservative Mixing at Stream Confluences. *Water Resources Research*, *59*(9), e2022WR034224. https://doi.org/10.1029/2022WR034224

Posit team. (2025). *RStudio: Integrated Development Environment for R* (2025.9.1.401). Posit Software, PBC. http://www.posit.co/

Ptacnik, R., Andersen, T., & Tamminen, T. (2010). Performance of the Redfield Ratio and a Family of Nutrient Limitation Indicators as Thresholds for Phytoplankton N vs. P Limitation. *Ecosystems*, *13*(8). https://doi.org/10.1007/s10021-010-9380-z

Qi, Y., Xie, Q., Wang, J. J., He, D., Bao, H., Fu, Q. L., Su, S., Sheng, M., Li, S. L., Volmer, D. A., Wu, F., Jiang, G., Liu, C. Q., & Fu, P. (2022). Deciphering dissolved organic matter by Fourier transform ion cyclotron resonance mass spectrometry (FT-ICR MS): from bulk to fractions and individuals. *Carbon Research 2022 1:1*, *1*(1), 1–22. https://doi.org/10.1007/S44246-022-00002-8

Ramette, A. (2007). Multivariate analyses in microbial ecology. *FEMS Microbiology Ecology*, *62*(2), 142–160. https://doi.org/10.1111/J.1574-6941.2007.00375.X

Raymond, P. A., Hartmann, J., Lauerwald, R., Sobek, S., McDonald, C., Hoover, M., Butman, D., Striegl, R., Mayorga, E., Humborg, C., Kortelainen, P., Dürr, H., Meybeck, M., Ciais, P., & Guth, P. (2013). Global carbon dioxide emissions from inland waters. *Nature 2013 503:7476*, *503*(7476), 355–359. https://doi.org/10.1038/nature12760

Redfield, A. C. (1960). The biological control of chemical factors in the environment. *Science Progress*, *11*, 150–170. https://pubmed.ncbi.nlm.nih.gov/24545739/

Ren, Y., Liu, S., Liu, L., Suo, C., Fu, R., Zhang, Y., Qiu, Y., & Wu, F. (2024). Deciphering the molecular composition and sources of dissolved organic matter in urban rivers based on optical spectroscopy and FT-ICR-MS analyses. *Carbon Research*, *3*(1), 1–14. https://doi.org/10.1007/S44246-024-00151-Y/FIGURES/7

Roddick, J. A., & Woodsworth, G. J. (2006). *Geology, Bute Inlet, British Columbia*. https://doi.org/10.4095/221570

Sahoo, I., Kondamudi, R. B., Tatiparthi, S., Siddela, D. V., & Rama Chandra Ganesh, P. (2025). Seasonal variation in the diversity of Holoplankton and Meroplankton in relation with primary productivity and physicochemical parameters in the nearshore regions of the Visakhapatnam Coast, India. *Advances in Oceanography and Limnology*, *16*(1). https://doi.org/10.4081/AIOL.2025.13309

Seelen, E. A., Gleich, S. J., Kumler, W., Anderson, H. S., Bian, X., Björkman, K. M., Caron, D. A., Dyhrman, S. T., Ferrón, S., Finkel, Z. V., Haley, S. T., Hu, Y. Y., Ingalls, A. E., Irwin, A. J., Karl, D. M., Kong, K. P., Lowenstein, D. P., Salazar Estrada, A. E., Townsend, E., … John, S. G. (2025). Nitrogen and phosphorus differentially control marine biomass production and stoichiometry. *Nature Communications*, *16*(1), 5713. https://doi.org/10.1038/s41467-025-61061-0

Shen, Y., & Benner, R. (2018). Mixing it up in the ocean carbon cycle and the removal of refractory dissolved organic carbon. *Scientific Reports 2018 8:1*, *8*(1), 2542-. https://doi.org/10.1038/s41598-018-20857-5

Singer, D., Seppey, C. V. W., Lentendu, G., Dunthorn, M., Bass, D., Belbahri, L., Blandenier, Q., Debroas, D., de Groot, G. A., de Vargas, C., Domaizon, I., Duckert, C., Izaguirre, I., Koenig, I., Mataloni, G., Romina Schiaffino, M., Mitchell, E. A. D., Geisen, S., & Lara, E. (2021). Protist taxonomic and functional diversity in soil, freshwater and marine ecosystems. *ENVIRONMENT INTERNATIONAL*, *146*. https://doi.org/10.1016/j.envint.2020.106262

Sipler, R. E., & Bronk, D. A. (2015). Dynamics of Dissolved Organic Nitrogen. In *Biogeochemistry of Marine Dissolved Organic Matter: Second Edition* (pp. 127–232). Elsevier Inc. https://doi.org/10.1016/B978-0-12-405940-5.00004-2

Sipler, R. E., Kellogg, C. T. E., Connelly, T. L., Roberts, Q. N., Yager, P. L., & Bronk, D. A. (2017). Microbial community response to terrestrially derived dissolved organic matter in the coastal Arctic. *Frontiers in Microbiology*, *8*(JUN). https://doi.org/10.3389/fmicb.2017.01018

Sleighter, R. L., & Hatcher, P. G. (2008). Molecular characterization of dissolved organic matter (DOM) along a river to ocean transect of the lower Chesapeake Bay by ultrahigh resolution electrospray ionization Fourier transform ion cyclotron resonance mass spectrometry. *Marine Chemistry*, *110*(3–4), 140–152. https://doi.org/10.1016/j.marchem.2008.04.008

Slowikowski, K. (2024). ggrepel: Automatically Position Non-Overlapping Text Labels with "ggplot2" [R package ggrepel version 0.9.6]. *CRAN: Contributed Packages*. https://doi.org/10.32614/CRAN.package.ggrepel

Sreeharsha, R. V., & Venkata Mohan, S. (2024). Photosynthetic Microbes: Evolution, Classification, and Structural Physiology. *Microbial Photosynthesis*, 3–22. https://doi.org/10.1007/978-981-97-1253-3_1

St. Pierre, K. A., Hunt, B. P. V., Giesbrecht, I. J. W., Tank, S. E., Lertzman, K. P., Del Bel Belluz, J., Hessing-Lewis, M. L., Olson, A., & Froese, T. (2022). Seasonally and Spatially Variable Organic Matter Contributions From Watershed, Marine Macrophyte, and Pelagic Sources to the Northeast Pacific Coastal Ocean Margin. *Frontiers in Marine Science*, *9*, 863209. https://doi.org/10.3389/FMARS.2022.863209/BIBTEX

St. Pierre, K. A., Hunt, B. P. V., Tank, S. E., Giesbrecht, I., Korver, M. C., Floyd, W. C., Oliver, A. A., & Lertzman, K. P. (2021). Rain-fed streams dilute inorganic nutrients but subsidise organic-matter-associated nutrients in coastal waters of the northeast Pacific Ocean. *Biogeosciences*, *18*(10), 3029–3052. https://doi.org/10.5194/bg-18-3029-2021

St. Pierre, K. A., Oliver, A. A., Tank, S. E., Hunt, B. P. V., Giesbrecht, I., Kellogg, C. T. E., Jackson, J. M., Lertzman, K. P., Floyd, W. C., & Korver, M. C. (2020). Terrestrial exports of dissolved and particulate organic carbon affect nearshore

ecosystems of the Pacific coastal temperate rainforest. *Limnology and Oceanography*, *65*(11), 2657–2675. https://doi.org/10.1002/lno.11538

Tee, H. S., Waite, D., Lear, G., & Handley, K. M. (2021). Microbial river-to-sea continuum: gradients in benthic and planktonic diversity, osmoregulation and nutrient cycling. *Microbiome 2021 9:1*, *9*(1), 1–18. https://doi.org/10.1186/S40168-021-01145-3

Teixeira, I. G., Arbones, B., Frojan, M., Nieto-Cid, M., Alvarez-Salgado, X. A., Castro, C. G., Fernandez, E., Sobrino, C., Teira, E., & Figueiras, F. G. (2018). Response of phytoplankton to enhanced atmospheric and riverine nutrient inputs in a coastal upwelling embayment. *ESTUARINE COASTAL AND SHELF SCIENCE*, *210*, 132–141. https://doi.org/10.1016/j.ecss.2018.06.005

Vähätalo, A. V., Aarnos, H., Hoikkala, L., & Lignell, R. (2011). Photochemical transformation of terrestrial dissolved organic matter supports hetero- And autotrophic production in coastal waters. *Marine Ecology Progress Series*, *423*, 1–14. https://doi.org/10.3354/meps09010

Vargas, C. A., Martinez, R. A., San Martin, V., Aguayo, M., Silva, N., & Torres, R. (2011). Allochthonous subsidies of organic matter across a lake–river–fjord landscape in the Chilean Patagonia: Implications for marine zooplankton in inner fjord areas. *Continental Shelf Research*, *31*(3–4), 187–201. https://doi.org/10.1016/J.CSR.2010.06.016

Voss, M., Bange, H. W., Dippner, J. W., Middelburg, J. J., Montoya, J. P., & Ward, B. (2013). The marine nitrogen cycle: recent discoveries, uncertainties and the potential relevance of climate change. *Philosophical Transactions of the Royal Society B: Biological Sciences*, *368*(1621), 20130121. https://doi.org/10.1098/rstb.2013.0121

Walsh, J. C., Pendray, J. E., Godwin, S. C., Artelle, K. A., Kindsvater, H. K., Field, R. D., Harding, J. N., Swain, N. R., & Reynolds, J. D. (2020). Relationships between Pacific salmon and aquatic and terrestrial ecosystems: implications for ecosystem-based management. *Ecology*, *101*(9), e03060. https://doi.org/10.1002/ecy.3060

Wang, W., Tao, J., Yu, K., He, C., Wang, J., Li, P., Chen, H., Xu, B., Shi, Q., & Zhang, C. (2021). Vertical Stratification of Dissolved Organic Matter Linked to Distinct Microbial Communities in Subtropic Estuarine Sediments. *Frontiers in Microbiology*, *12*, 697860. https://doi.org/10.3389/FMICB.2021.697860/BIBTEX

Ward, N. D., Megonigal, J. P., Bond-Lamberty, B., Bailey, V. L., Butman, D., Canuel, E. A., Diefenderfer, H., Ganju, N. K., Goñi, M. A., Graham, E. B., Hopkinson, C. S., Khangaonkar, T., Langley, J. A., McDowell, N. G., Myers-Pigg, A. N., Neumann, R. B., Osburn, C. L., Price, R. M., Rowland, J., … Windham-Myers, L. (2020). Representing the function and sensitivity of coastal interfaces in Earth system models. In *Nature Communications* (Vol. 11, Number 1). https://doi.org/10.1038/s41467-020-16236-2

Wickham, H., Averick, M., Bryan, J., Chang, W., McGowan, L., François, R., Grolemund, G., Hayes, A., Henry, L., Hester, J., Kuhn, M., Pedersen, T., Miller, E., Bache, S., Müller, K., Ooms, J., Robinson, D., Seidel, D., Spinu, V., … Yutani, H. (2019). Welcome to the Tidyverse. *Journal of Open Source Software*, *4*(43), 1686. https://doi.org/10.21105/JOSS.01686

Wood, S. N. (2011). mgcv: Fast stable restricted maximum likelihood and marginal likelihood estimation of semiparametric generalized linear models. *Journal of the Royal Statistical Society. Series B: Statistical Methodology*, *73*(1), 3–36. https://doi.org/10.1111/j.1467-9868.2010.00749.x

Wu, X., Wu, L., Liu, Y., Zhang, P., Li, Q., Zhou, J., Hess, N. J., Hazen, T. C., Yang, W., & Chakraborty, R. (2018). Microbial interactions with dissolved organic matter drive carbon dynamics and community succession. *Frontiers in Microbiology*, *9*(JUN), 359717. https://doi.org/10.3389/fmicb.2018.01234

Yao, J., Chen, Z., Ge, J., & Zhang, W. (2024). Source-To-sink pathways of dissolved organic carbon in the river-estuary-ocean continuum: A modeling investigation. *Biogeosciences*, *21*(23), 5435–5455. https://doi.org/10.5194/BG-21-5435-2024

Yool, A., & Tyrrell, T. (2003). Role of diatoms in regulating the ocean's silicon cycle. *Global Biogeochemical Cycles*, *17*(4). https://doi.org/10.1029/2002gb002018

Yu, F., Zong, Y., Lloyd, J. M., Huang, G., Leng, M. J., Kendrick, C., Lamb, A. L., & Yim, W. W. S. (2010). Bulk organic δ13C and C/N as indicators for sediment sources in the Pearl River delta and estuary, southern China. *Estuarine, Coastal and Shelf Science*, *87*(4), 618–630. https://doi.org/10.1016/j.ecss.2010.02.018

Zeglin, L. H. (2015). Stream microbial diversity in response to environmental changes: Review and synthesis of existing research. *Frontiers in Microbiology*, *6*(MAY), 128252. https://doi.org/10.3389/FMICB.2015.00454/ABSTRACT

Zhang, H., Xing, D., Wu, Y., Jin, R., Liu, D., & Deines, P. (2023). Editorial: Microbial ecology and function of the aquatic systems. *Frontiers in Microbiology*, *13*, 1109221. https://doi.org/10.3389/FMICB.2022.1109221

Zoccarato, L., & Grossart, H. P. (2019). *Relationship Between Lifestyle and Structure of Bacterial Communities and Their Functionality in Aquatic Systems* (pp. 13–52). https://doi.org/10.1007/978-3-030-16775-2_2

Statements and Declarations

Conflict of Interest

The authors declare no conflicts of interest relevant to this study.

Data Availability Statement

The original datasets and coding associated with the results can be retrieved at (TBD).

Chapter 3: Thesis Conclusions

Key scientific takeaways

This study fills a critical gap by integrating concepts and techniques from limnology and oceanography to examine high-resolution dynamics of nutrient (nitrogen, phosphorus, and silica), organic matter, and microbial (prokaryote and eukaryote) community composition across small coastal river plumes. By adopting an estuary lens, it: (1) delineates the extent of the plume from a small rain-dominated system; (2) quantifies nutrient concentrations and characterizes organic matter characteristics across the plume; and (3) links microbial community composition and activity to these biogeochemical trends. Together, these aimed to address the guiding research question: *How do riverine exports of nutrients and organic matter influence the putatively active microbes and biogeochemical cycling across small river plumes of the NPCTR?*

The results described herein demonstrate that riverine export of nutrients and organic matter, specifically changes in organic carbon dynamics and salinity, actively shaped putatively active microbial at freshwater-ocean interfaces downstream of small rain-dominated riverine coastal watersheds in the NPCTR. Although functional traits or niches were not directly characterized, biogeochemical-microbial coupling strongly support salinity and organic matter as the dominant drivers for shaping these interfaces.

Most importantly, this study detects fine-scale (tens of centimeter or less) gradients in physical, geochemical, and microbial variables at high-resolution lens often overlooked in exclusively freshwater and marine sciences (Dagg et al., 2004; Hunt et al., 2024; O'Donnell et al., 2008). Despite being limited to the surface, these freshwater exports display patterns in chemistry and microbial community composition and activity that align with trends in larger river plumes such as the Fraser or Eel Rivers (Hunt et al., 2024). This highlights that small river plumes are not merely diluted versions of larger systems (St. Pierre et al., 2021), but need to be considered in their own right as distinct ecosystems. Methodologically, this research demonstrates the value of interdisciplinary techniques, by coupling nutrient and organic matter chemistry with amplicon sequencing along salinity gradients, advancing our current understanding and frameworks within not only the NPCTR (Giesbrecht et al., 2022, 2025) but small river plumes globally.

Limitations and trade-offs

The field portion of the study was planned to capture the period of highest freshwater influence (i.e., highest rainfall and lowest oceanic upwelling) for the northeast Pacific Ocean. Fieldwork was initially planned for January 2022, then postponed due to a major atmospheric river (rainfall) event and rescheduled for February 2022 (Hunt et al., 2024; Teixeira et al., 2018). However, due to rising temperatures and a changing climate, an early spring bloom occurred during the sampling period (NASA

Worldview, 2022). This introduced unexpected biological activity, with evidence of algal growth due to the newly available nutrients after winter dormancy (Gobler, 2020). Thus, identifying the top 30 eukaryotes and prokaryotes proved a limiting metric, as the results were overwhelmingly skewed toward autotrophic orders, associated with algal blooms (Gobler, 2020; Howard et al., 2022).

Sampling took place over a discrete period, such that these results are not indicative of seasonal or temporal variation and should instead be perceived as a snapshot of the dynamics during a season of high freshwater influence. Another sampling limitation is the lack of replicates at each depth within the plume. Though Hyacinthe Creek was sampled six times in the week leading up to the ocean sampling, each location in the plume only had a single measurement due to limited resources and time constraints, preventing a robust assessment of variability. An example of where this may have influenced the results is the total nitrogen (TN) measurement 780 m from the creek mouth at 50 cm depth. The original measurement was significantly higher compared to the dataset, with a concentration of 104.96 μM, compared to 27.34 μM and 3.59 μM for DN and PN, respectively. Due to this discrepancy, PN and DN were summed to represent this value instead of the original measurement. Furthermore, due to the sampling taking place at low tide in Hyacinthe Bay, no measurement for 50 cm could be taken from site 1 (79 m from creek mouth) as the tide was going out.

Future Directions

Building on the limitations and insights presented in this study, future work should continue to adapt and apply this framework across other regions of the NPCTR. Extending this analysis would aid in evaluating the ubiquity and consistency of the patterns observed here, further developing our understanding of small river plume dynamics across freshwater-ocean interfaces.

Several key questions emerged from this research: *(1) How do patterns observed in these small river plumes compare to other biomes globally (e.g., tropical vs temperate systems)? (2) What are the functional characteristics of the microbial taxa involved, and how might they interact with shifting these biogeochemical parameters across salinity gradients?* Approaches such as combining PyCrust with amplicon sequencing could give insight into functional linkages in coastal zones (Singer et al., 2021; Zoccarato & Grossart, 2019). *(3) Can similar approaches applied to other NPCTR rain-dominated watershed types (i.e., RMN, RHN, RLN, RMC, RLC, RHS, and RHC) reveal whether these findings are unique to the rain hills-central type or broadly representative of rain-dominated coastal ecosystems?* Lastly, at larger temporal scales, *(4) how does seasonal variation in freshwater exports impacts the spatial extent and geochemical structure of small river plumes?*

If replicating this work, increasing replicates would strengthen and enhance statistical robustness, allowing for averaged comparisons across gradients and avoiding outlier bias (Buttigieg & Ramette, 2014; Paliy & Shankar, 2016). Additionally,

expanding sampling to small watersheds within Quadra Island and neighbouring sites would allow ubiquity analysis of these gradients across geomorphologically similar ecosystems. The most promising future directions lies in the integration of cross-disciplinary, high-resolution approaches to estuarine ecosystems, by combining biogeochemistry, salinity mapping, and microbial sequencing to small-scale freshwater-ocean interfaces. This framework sets a precedent for future experimentation and emphasizes the need to observe dynamics at a fine scale when studying small river plumes.

Reflections on the research process

This research process highlighted the non-linear nature of science and the significant role of collaboration. Although I was not involved in the original study design or fieldwork, I was deeply engaged in constructing the scientific narrative through data management and analysis, collaboration with co-authors, writing, and figure development. This experience reinforced that environmental science is seldom a linear process and always depends on extensive partnerships. Rarely does research progress from a single question to a single answer; more often, it begins with one question that rapidly develops into many.

One of the most surprising aspects of this project was how much it evolved from my original plan. When I began as an Honour's student, I set out to conduct a meta-analysis of freshwater-ocean connections at coastal interfaces by integrating multiple small-scale studies. However, over time, a clear knowledge gap emerged: beyond traditional estuarine research, most oceanography and limnology studies treat coastal environments and freshwater watersheds independently, leaving their interactions poorly characterized, especially at this fine scale. This disconnect stems largely from to the technical and logistical barriers that divide limnological and oceanographic research. As a result, the focus of my research shifted to analyzing an underutilized biogeochemical dataset collected at a freshwater-marine interface of a small river plume in the NPCTR, providing a unique opportunity to bridge this knowledge gap.

Working with these datasets presented substantial conceptual and analytical challenges. It required learning multiple analytical approaches and determining how to synthesize a large volume of data into a cohesive narrative, which describes processes within highly dynamic, small, rain-dominated river plumes. Incorporating key concepts from environmental chemistry, environmental microbiology, limnology and oceanography was a difficult but rewarding learning curve. The process involved continual refinement of research questions, extensive literature review, and recognition of when external expertise was needed. Even in the final stages, feedback from supervisors, co-authors and peer-review emphasized that scientific understanding is always evolving and that there is always more to question, explore, and refine.

Several limitations and trade-offs influenced how the data could be analyzed and presented. The data were inherently complex, and determining which parameters were most appropriate for inclusion required two years of refinement. Behind every figure, there were countless iterations and failed attempts, alongside the tedious process of learning analytical tools such

as RStudio and ArcGIS Pro. These experiences reinforced the value of persistence and perspective: many challenges that appeared to be insurmountable often resolved themselves over time, reflection, and revision. Rather than treating failure as a major setback, it became a critical part of refining my approach and redirecting analysis.

Overall, the research process has contributed significantly to my development as an environmental scientist. Over the past two years, I have developed skills in critical thinking, project management, collaboration, coding, and scientific writing. This thesis has prepared me for future research and applied work by advancing not only my technical skills, by also my understanding of estuaries and aquatic ecology. Most importantly, the experience has shaped how I will approach future interdisciplinary research, by involving multiple perspectives, constructive feedback, and collaborative problem-solving. Moving forward, I will continue to approach ecosystems not as isolated units, but as interconnected pieces of the larger puzzle of environmental and earth sciences.

Closing remarks

Small rain-dominated river watersheds in the NPCTR contribute supplementary biogeochemical variables to coastal zones, further impacting coastal processes and productivity, with organic matter and salinity dynamics driving the primary microbial community gradients. Overall, this study supports existing findings on river plumes at the coastal margin at a high resolution (centimeter deep) scale, a lens typically overlooked in traditional oceanography and limnology. This study opens doors for developing new interdisciplinary frameworks for studying these key freshwater-ocean interfaces. We ultimately suggest the integration of high-resolution freshwater lens' into future estuarine research of small river plumes, and the integration of cross-realm interdisciplinary perspectives when addressing scientific questions in aquatic ecosystem ecology.

Appendix: Supplementary Figures, Tables, and Methodology

Supplementary Figures

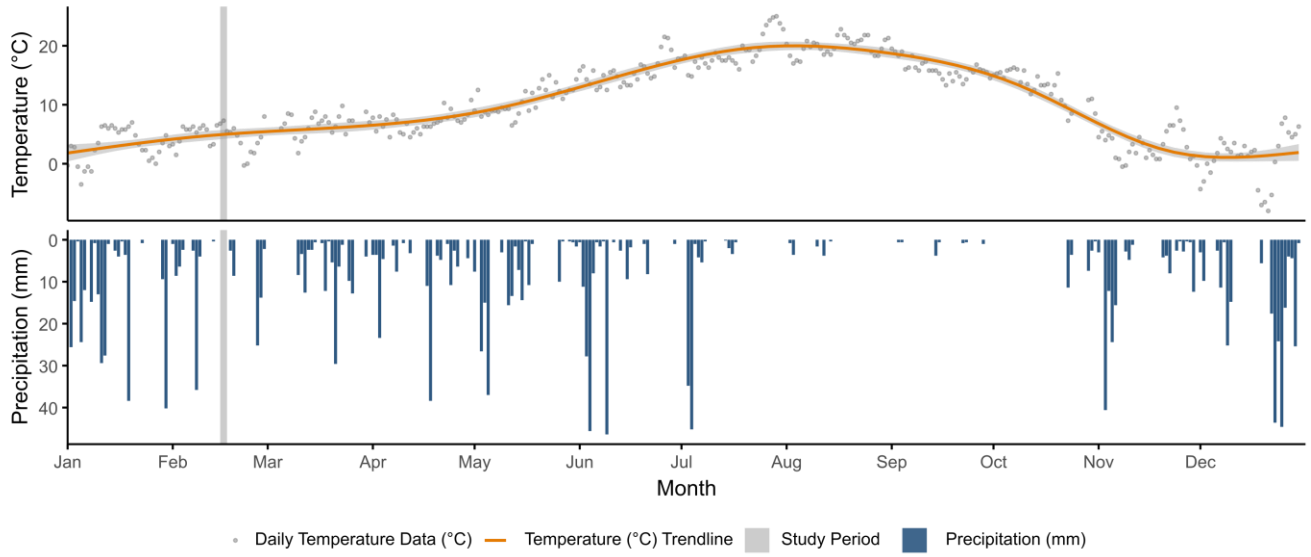

Figure A1: Daily mean air temperature (°C) and total precipitation (mm) from the Heriot Bay SE Environment Canada monitoring station (Climate ID: 1023462) for the 2022 calendar year (CCN, 2022).
The shaded bands denote the sampling period (July 16-18th, 2022).

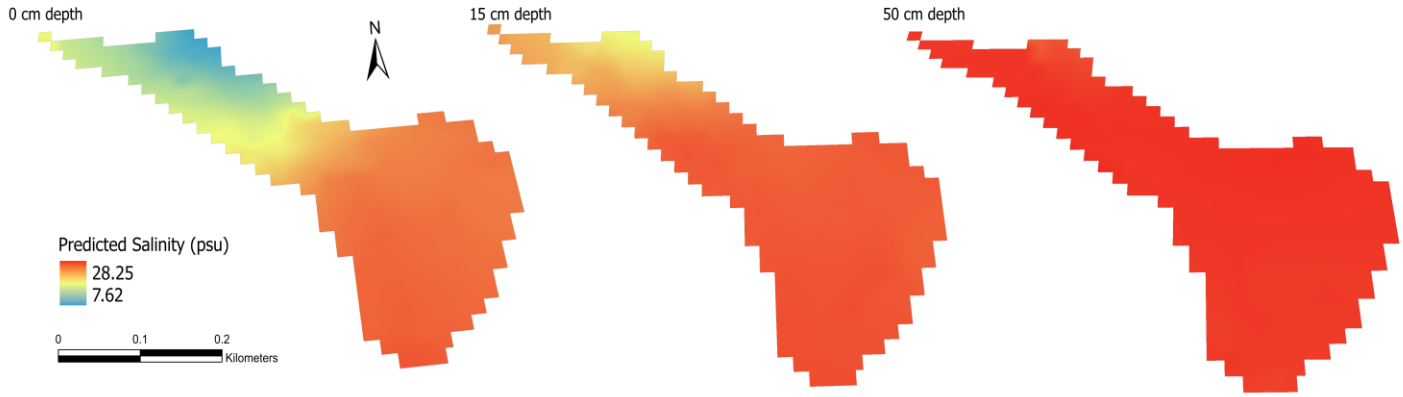

Figure A2: Three-dimensional salinity reconstruction of the estuarine plume.
3D Empirical Bayesian Kriging Interpolated salinity (PSU) with a vertical exaggeration of 2.44, highlighting horizontal and vertical structure of the plume, with warmer colors indicating higher salinity and cooler colors indicating fresher, plume-influenced waters.

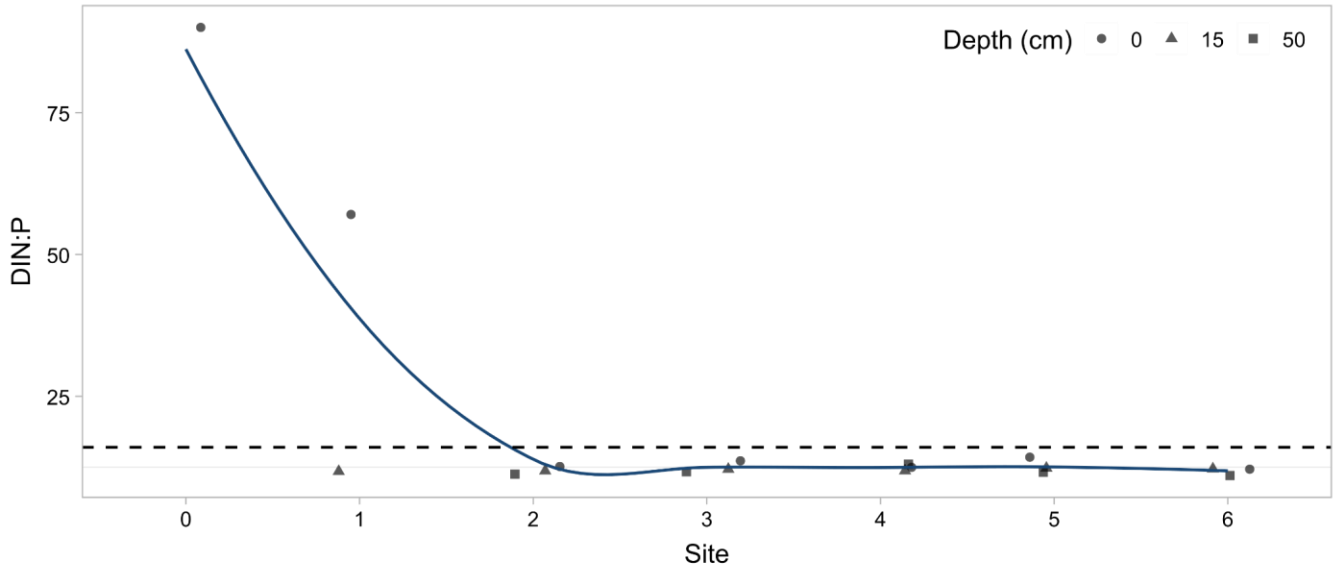

Figure A3: Dissolved inorganic nitrogen to total phosphorus (DIN:TP) ratios across the freshwater–marine transect
DIN:TP ratios plotted by site (0 through 6) and depth (0, 15, and 50 cm), illustrating spatial patterns in nutrient limitation along the salinity gradient. The horizontal dashed line at a DIN:TP ratio of 16 marks the canonical Redfield ratio, distinguishing nitrogen-limited (<16) from phosphorus-limited (>16) conditions.

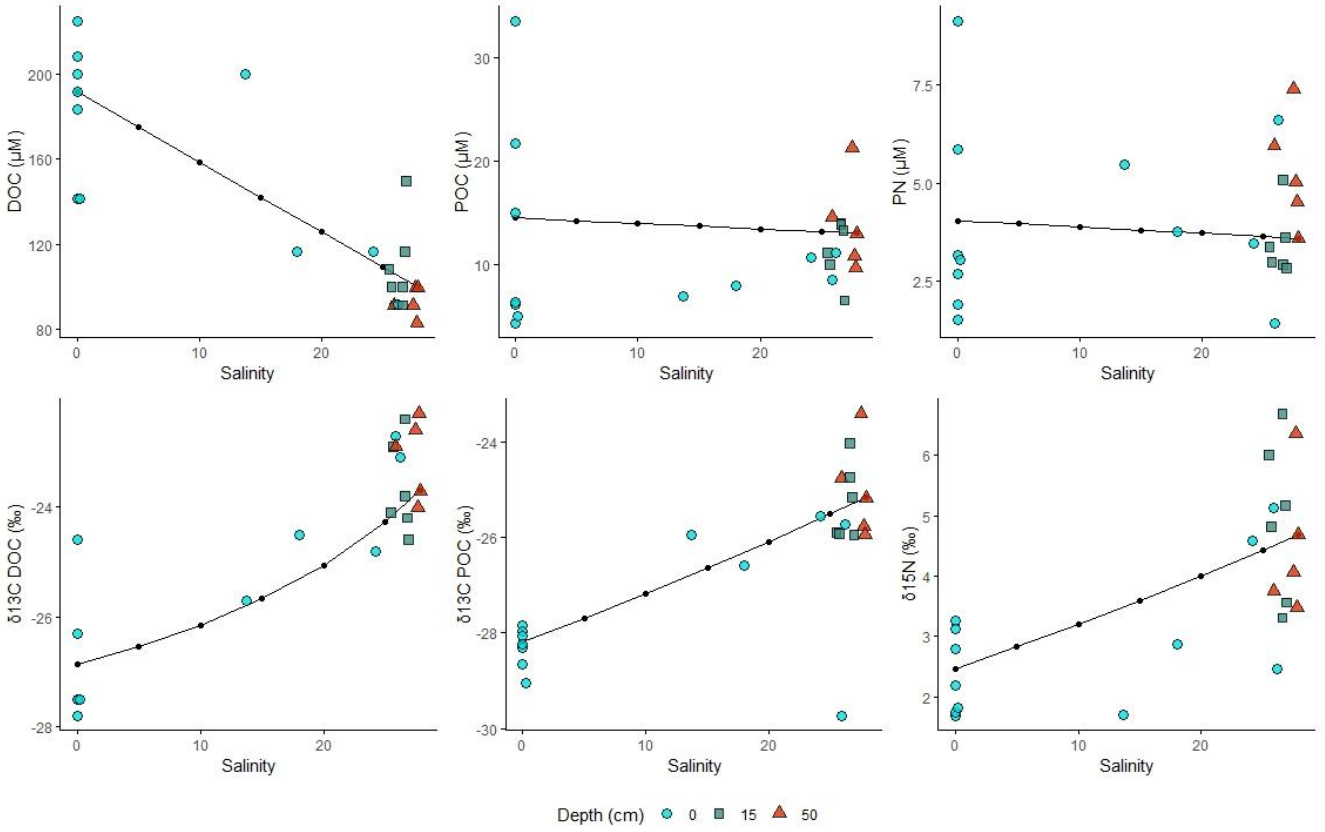

Figure A4: Deviations from conservative mixing for carbon and nitrogen pools and isotopes across the salinity gradient
Measured versus conservative-mixing-predicted values are shown for DOC, POC, PN, δ^{13}C-DOC, δ^{13}C-POC, and δ^{15}N-PN, interpolated across salinities ranging from freshwater (0 PSU) to marine (27.9 PSU). Deviations from theoretical mixing lines indicate biogeochemical transformations such as remineralization, selective sorption, and microbial processing within the estuarine transition zone.

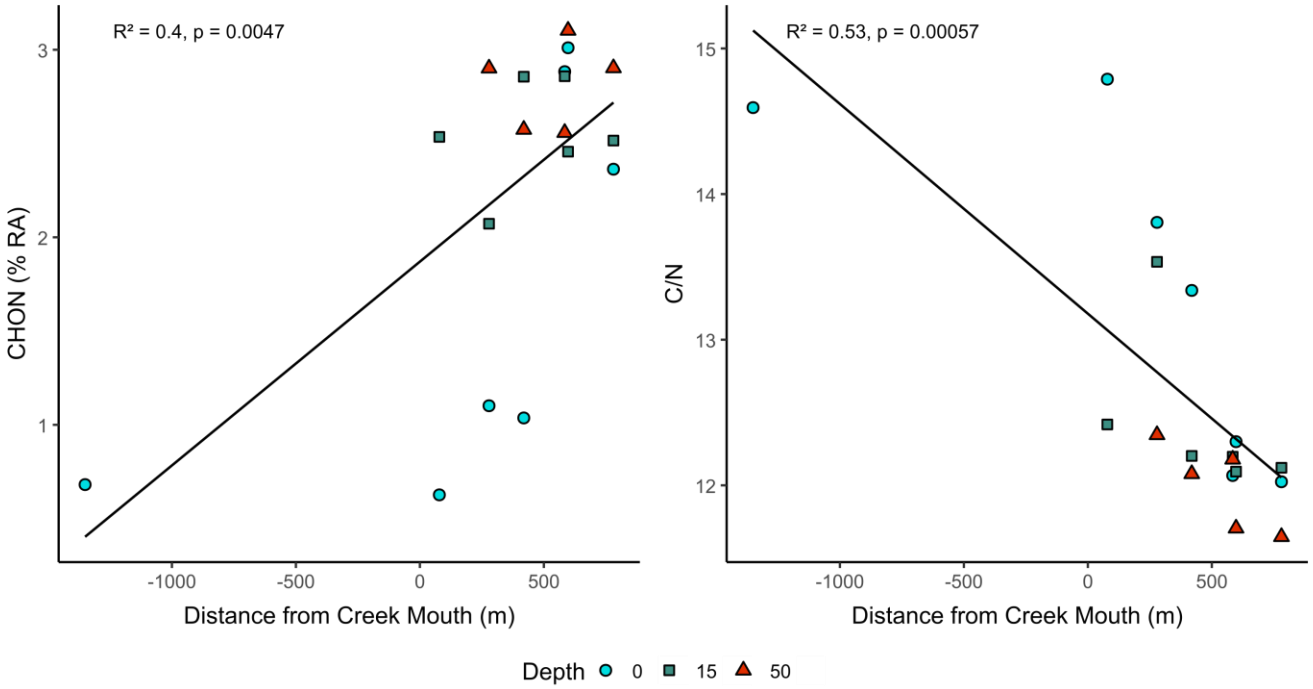

Figure A5: Elemental ratios and heteroatom content derived from ultrahigh-resolution mass spectrometry. Bulk CHON composition and calculated C/N ratios based on molecular formulae from FT-ICR-MS analyses of dissolved organic matter (DOM) samples collected with increasing distance from the creek mouth (m) at depths of 0, 15, and 50 cm.

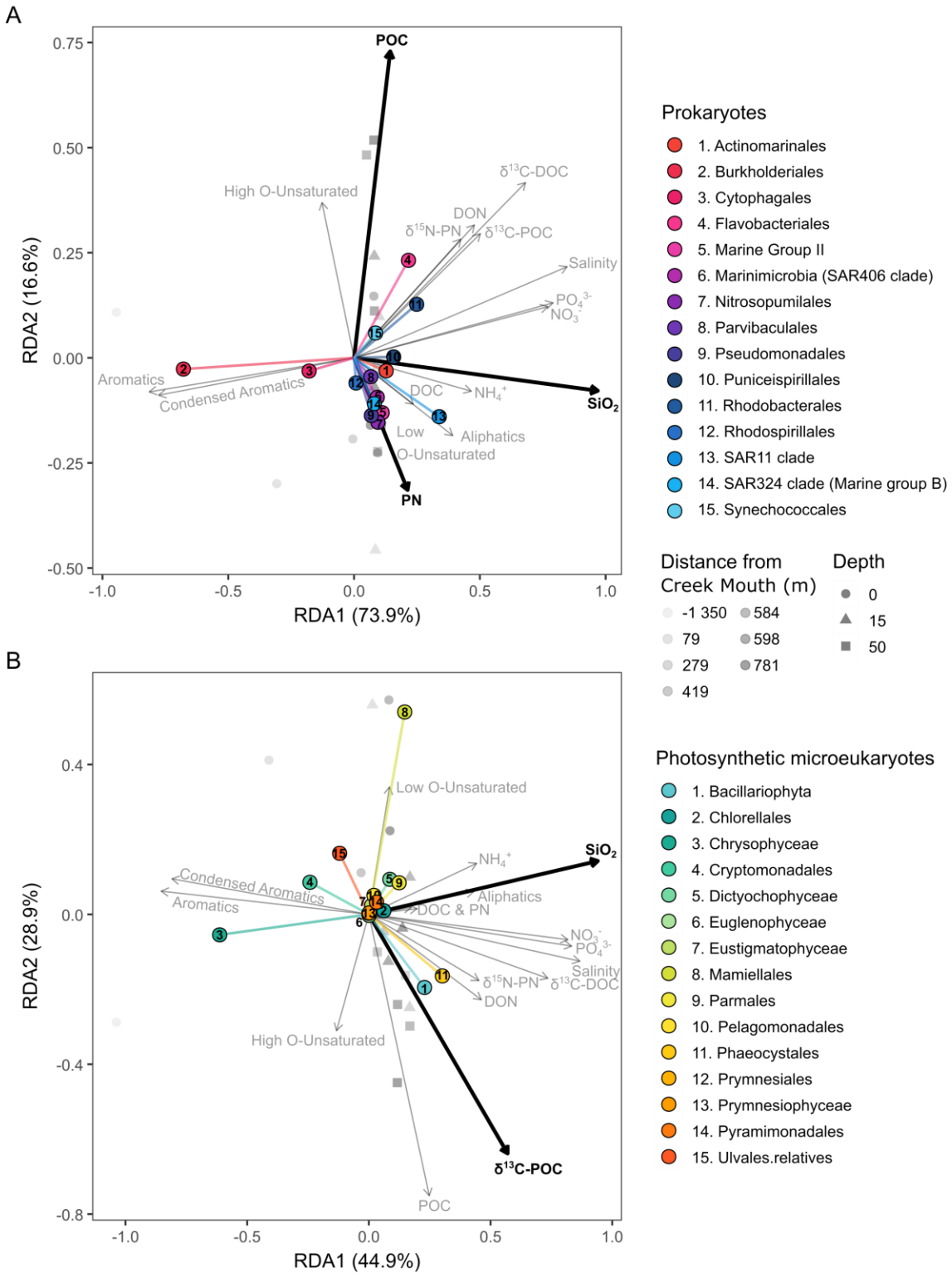

Figure A6: Redundancy analysis (RDA) of microbial community composition (DNA) and environmental drivers.
(A) RDA ordinations of prokaryotic community composition by proxy of DNA relative abundance constrained by physicochemical and organic matter variables (Salinity, DOC, POC, δ^{13}C-DOC, δ^{13}C-POC, δ^{15}N, PN, DON, NO_3^-, NH_4^+, PO_4^{3-}, SiO_2, aliphatics, aromatics, condensed aromatics, low-O unsaturated, and high-O unsaturated compounds) with axes showing the percentage of variance explained. (B) RDA ordinations of eukaryotic community composition by proxy of DNA relative abundance showing the response of major phytoplankton and plastid groups to the same suite of environmental variables. Coloured points represent dominant prokaryotic and eukaryotic orders, grey symbols indicate sampling depth and distance from the creek mouth (m), and black vectors highlight environmental gradients, with the significant variables in bold.

Supplementary Tables

Table A1: Metadata and physicochemical characteristics for Hyacinthe Creek and Hyacinthe Bay sampling stations including geographic coordinates, distance from the creek mouth, number of replicates, sampling depth, temperature, salinity, specific conductivity, turbidity, and discharge.

Site	Latitude (°)	Longitude (°)	Distance from Creek Mouth (m)*	Replicates	Depth (cm)	Temperature (°C)	Salinity (PSU)	Specific conductivity (µS/cm)	Turbidity	Discharge (m^3/s)
0	50.13338	-125.254	-1350.21	6	0	4.4	0	32.91667	2.891667	0.0447
1	50.12922	-125.239	78.55	1	0	-	0.2	410.2	-	-
1	50.12922	-125.239		1	15	-	26.9	42236	-	-
2	50.12876	-125.236	278.87	1	0	-	13.7	22766	-	-
2	50.12876	-125.236		1	15	-	26.6	41875	-	-
2	50.12876	-125.236		1	50	-	27.9	43556	-	-
3	50.12811	-125.234	419.02	1	0	-	18	29165	-	-
3	50.12811	-125.234		1	15	-	26.8	42056	-	-
3	50.12811	-125.234		1	50	-	27.8	43465	-	-
4	50.12686	-125.232	584.09	1	0	6.7	25.9	40000	-	-
4	50.12686	-125.232		1	15	6.7	25.7	40335	-	-
4	50.12686	-125.232		1	50	6.7	25.9	40060	-	-
5	50.12711	-125.232	597.65	1	0	-	24.2	38296	-	-
5	50.12711	-125.232		1	15	-	25.5	40165	-	-
5	50.12711	-125.232		1	50	-	27.7	43290	-	-
6	50.12569	-125.23	780.71	1	0	-	26.2	41115	-	-
6	50.12569	-125.23		1	15	-	26.6	41677	-	-
6	50.12569	-125.23		1	50	-	27.5	42987	-	-

** Estimated using the measure tool in ArcGISPro.*

Table A2: Analytical methods and laboratories by chemical constituent listing analyte names, sampling dates, units, data availability (freshwater, marine, or both), instruments or formulas, analytical laboratory, detection limits, and analytical error.

Constituent	Name	Sampling	Unit	Instrument/Formula	Analytical Lab[a]	Detection limit	Error
TN	Total nitrogen	11/03/2022	µg/L	Lachat QC8500 FIA Analyzer	BASL	0.500	0.50%
PN	Particulate nitrogen	25/07/2022	µg	Elementar MICRO cube + VisION IRMS	UCDavis	100	-
TDN	Total dissolved nitrogen	11/03/2022	µg/L	Lachat QC8500 FIA Analyzer	BASL	0.500	0.50%
NH_4^+	Ammonium	11/03/2022	µg/L	Lachat QC8500 FIA Analyzer	BASL	0.214	0.50%
$NO_3^- + NO_2^-$	Combined nitrate-nitrite	01/31/2023	µM	Lachat QC8500 FIA Analyzer	U.B.C.	0.036	0.50%
DIN	Dissolved inorganic nitrogen	-	-	DIN = $NH_4^+ + NO_3^- + NO_2^-$	-	-	-
DON	Dissolved organic nitrogen	-	-	DON = TDN - DIN	-	-	-
δ15N	Particulate Nitrogen isotopes	25/07/2022	‰	Elementar MICRO cube + VisION IRMS	UCDavis	-	0.3 ‰
TP	Total phosphorous	11/03/2022	µg/L	Lachat QC8500 FIA Analyzer	BASL	0.045	0.50%
TDP	Total dissolved phosphorous	11/03/2022	µg/L	Lachat QC8500 FIA Analyzer	BASL	0.058	0.50%
PO_4^{3-}	Phosphate	01/31/2023	µM	Lachat QC8500 FIA Analyzer	U.B.C.	0.032	0.50%
DOC	Dissolved organic carbon	23/03/2022	ppm	OI Analytical TIC-TOC 1030 + DeltaPlus XP IRMS	JVSIL	0.1	0.5 ppm
δ^{13}C-DOC	Dissolved organic carbon isotopes	23/03/2023	‰	OI Analytical TIC-TOC 1030 + DeltaPlus XP IRMS	JVSIL	-	0.2 ‰
POC	Particulate organic carbon	25/07/2022	µg	Elementar MICRO cube + VisION IRMS	UCDavis	100	-
δ^{13}C-POC	Particulate Carbon isotopes	25/07/2022	‰	Elementar MICRO cube + VisION IRMS	UCDavis	-	0.2‰
TOC	Total organic carbon	-	-	TOC = POC + DOC	-	-	-
SiO2	Silica	01/31/2023	µM	Lachat QC8500 FIA Analyzer	U.B.C.	0.1	0.50%

[a] BASL, Biogeochemical Analytical Service Laboratory in the Department of Biological Sciences at the University of Alberta (Edmonton, AB, Canada). U.B.C., Marine Zooplankton and Micronekton Laboratory in the Department of Earth Oceans and Atmospheric Sciences (Vancouver, B.C., Canada). JVSIL, Ján Veizer Stable Isotope Facility at the University of Ottawa (Ottawa, ON, Canada). UCDavis, University of California Davis Stable Isotope Facility (Davis, CA, USA).

Table A3: Carbon and nutrient and DOM ANOVA results across horizontal and vertical salinity gradients showing P values for effects of site (i.e., distance), depth, and their interaction on Salinity, TN, PN, DN, NH_4^+, NO_3^- DON, DIN, PO_4^{3-}, SiO_2, DOC, POC, isotopic signatures, DIN:P, and each FT-ICR-MS-derived compound class across all samples. These values are calculated based on a Model II ANOVA.

Parameter	Site	Depth
Physical parameters		
Salinity	0.109	0.066
Nutrient and Carbon Concentrations		
TN	0.344	0.012
PN	0.471	0.667
DN	0.138	0.019
NH_4^+	0.409	0.839
DIN	0.328	0.092
DON	0.150	0.060
NO_{3-}	0.307	0.078
δ^{15}N-PN	0.163	0.047
PO_4^{3-}	0.252	0.063
SiO_2	0.002	0.561
DOC	0.529	0.533
δ^{13}C-DOC	0.011	0.048
POC	0.101	0.041
δ^{13}C-POC	0.207	0.033
DIN.P	0.022	0.306
DOM compound classes		
Aliphatic	0.053	0.410
Condensed Aromatics	0.269	0.294
Aromatic	0.212	0.206
Low-O Unsaturated	0.478	0.729
High-O Unsaturated	0.210	0.633

Table A4: Summary statistics for carbon and nutrient concentrations/signatures, stoichiometric ratios, and DOM compound classes relative abundances including minimum, maximum, median, mean, and standard deviation for TN, PN, DN, NH_4^+, NO_3^- DON, DIN, PO_4^{3-}, SiO_2, DOC, POC, isotopic signatures, DIN:P, and each FT-ICR-MS-derived compound class across all samples.

Parameter	Min	Max	Median	Mean	STD
Nutrient and Carbon concentrations/signatures					
TN	8.92	38.62	31.74	28.80	9.11
PN	1.45	9.10	3.47	3.88	1.88
DN	9.85	35.20	30.13	27.27	7.53
NH_4^+	0.11	1.07	0.57	0.53	0.29
DIN	5.52	25.94	22.26	20.13	5.98
DON	0.60	11.41	7.93	7.14	2.53
NO_3^-	5.42	24.86	21.66	19.60	5.81
δ^{15}N-PN	1.70	6.69	3.92	4.05	1.49
PO_4^{3-}	0.07	2.22	1.83	1.62	0.64
SiO_2	13.80	55.30	51.42	48.63	10.01
TOC	97.29	211.00	113.74	124.00	29.18
DOC	83.26	199.83	99.92	112.87	29.16
δ^{13}C-DOC	-27.50	-22.30	-23.90	-24.04	1.48
POC	4.99	21.33	10.99	11.13	3.73
δ^{13}C-POC	-29.73	-23.42	-25.84	-25.98	1.60
DIN:P	11.03	90.04	12.18	19.05	20.63
DOM Compound Classes Relative Abundance					
Aliphatic	2.55	47.36	14.87	19.92	13.01
Condensed Aromatics	0.17	3.67	0.53	0.82	0.91
Aromatic	0.32	14.42	2.24	3.47	3.98
Low-O Unsaturated	21.48	49.80	36.28	35.25	6.25
High-O Unsaturated	10.08	53.86	43.73	39.75	10.59

Table A5: CHON & C/N calculated measurements from FT-ICR-MS DOM characterisation.
CHON composition and C/N ratios derived from FT-ICR-MS molecular formulae for dissolved organic matter, reported by site, depth, distance from the creek mouth (m), and salinity (PSU), with corresponding regression R^2 and P values for relationships between CHON, C/N, and salinity along the transect.

Site	Depth	Distance (m)	Salinity (PSU)	CHON (% Relative Abundance)	C/N
0	0	-1350.21	0	0.68	14.59
1	0	78.55	0.2	0.63	14.79
1	15	78.55	26.9	2.54	12.42
2	0	278.87	13.7	1.10	13.81
2	15	278.87	26.6	2.07	13.53
2	50	278.87	27.9	2.90	12.35
3	0	419.02	18	1.04	13.34
3	15	419.02	26.8	2.86	12.20
3	50	419.02	27.8	2.57	12.08
4	0	584.09	25.9	2.88	12.07
4	15	584.09	25.7	2.86	12.20
4	50	584.09	25.9	2.56	12.18
5	0	597.65	24.2	3.01	12.30
5	15	597.65	25.5	2.46	12.09
5	50	597.65	27.7	3.10	11.71
6	0	780.71	26.2	2.36	12.02
6	15	780.71	26.6	2.52	12.12
6	50	780.71	27.5	2.90	11.65
R^2 value				0.403	0.534
p-value				0.005	0.0006

Table A6: Top eukaryotic and prokaryotic orders by mean relative abundance (RA) and percent relative abundance (RA) listing the 30 most abundant prokaryotic and microeukaryotic orders in DNA and RNA datasets with "Other" category for all other orders.

	DNA			RNA		
Rank	**Order**	**Mean RA**	**% RA**	**Order**	**Mean RA**	**% RA**
Prokaryotes						
1	*Flavobacteriales*	0.2287	22.87	*Flavobacteriales*	0.3055	30.55
2	*SAR11 clade*	0.2114	21.14	*Rhodobacterales*	0.1378	13.78
3	*Pseudomonadales*	0.1232	12.32	*Pseudomonadales*	0.1275	12.75
4	*Rhodobacterales*	0.1224	12.24	*Synechococcales*	0.1151	11.51
5	*Burkholderiales*	0.0653	6.53	*Burkholderiales*	0.0819	8.19
6	*Nitrosopumilales*	0.0360	3.60	*SAR11 clade*	0.0451	4.51
7	*Synechococcales*	0.0268	2.68	*Puniceispirillales*	0.0322	3.22
8	*Puniceispirillales*	0.0249	2.49	*Rhodospirillales*	0.0138	1.38
9	*Actinomarinales*	0.0183	1.83	*SAR324 clade (Marine group B)*	0.0120	1.20
10	*Parvibaculales*	0.0150	1.50	*Nitrosopumilales*	0.0102	1.02
11	*Marine Group II*	0.0140	1.40	*Parvibaculales*	0.0067	0.67
12	*Marinimicrobia (SAR406 clade)*	0.0115	1.15	*Cytophagales*	0.0057	0.57
13	*SAR324 clade (Marine group B)*	0.0096	0.96	*Marinimicrobia (SAR406 clade)*	0.0054	0.54
14	*Rhodospirillales*	0.0091	0.91	*Marine Group II*	0.0025	0.25
15	*Cytophagales*	0.0049	0.49	*Actinomarinales*	0.0013	0.13
	Other	0.0790	7.90	Other	0.0973	9.73
Photosynthetic microeukaryotes						
1	*Phaeocystales*	0.4508	45.08	*Bacillariophyta*	0.6046	60.46
2	*Bacillariophyta*	0.2670	26.70	*Phaeocystales*	0.2314	23.14
3	*Mamiellales*	0.1174	11.74	*Cryptomonadales*	0.0701	7.01
4	*Cryptomonadales*	0.0793	7.93	*Mamiellales*	0.0351	3.51
5	*Chrysophyceae*	0.0348	3.48	*Chrysophyceae*	0.0221	2.21
6	*Parmales*	0.0163	1.63	*Ulvales relatives*	0.0145	1.45
7	*Dictyochophyceae*	0.0135	1.35	*Dictyochophyceae*	0.0130	1.30
8	*Ulvales relatives*	0.0112	1.12	*Parmales*	0.0052	0.52
9	*Pyramimonadales*	0.0041	0.41	*Pyramimonadales*	0.0023	0.23
10	*Chlorellales*	0.0038	0.38	*Pelagomonadales*	0.0007	0.07
11	*Pelagomonadales*	0.0010	0.10	*Chlorellales*	0.0006	0.06
12	*Eustigmatophyceae*	0.0006	0.06	*Eustigmatophyceae*	0.0003	0.03
13	*Prymnesiales*	0.0001	0.01	*Prymnesiales*	0.0002	0.02
14	*Euglenophyceae*	0.0001	0.01	*Euglenophyceae*	0.0000	0.00
15	*Prymnesiophyceae*	0.0000	0.00	*Prymnesiophyceae*	0.0000	0.00

Table A7: Microbial community ANOVA results for dominant orders
Two-way (Model II) ANOVA results showing p values for effects of site (i.e., distance) and depth on DNA- and RNA-based relative abundances of key prokaryotic and photosynthetic microeukaryotic orders, along with residual degrees of freedom.

Order	Site (DNA)	Depth (DNA)	Site (RNA)	Depth (RNA)	Residuals
Prokaryotes					
Actinomarinales	0.054	0.216	0.573	0.181	NA
Burkholderiales	0.000*	0.311	0.004	0.205	1638
Cytophagales	0.000*	0.228	0.010	0.134	360
Flavobacteriales	0.060	0.112	0.054	0.126	1980
Marine Group II	0.450	0.268	0.811	0.596	252
Marinimicrobia (SAR406 clade)	0.045	0.031	0.297	0.280	180
Nitrosopumilales	0.004	0.698	0.403	0.820	108
Parvibaculales	0.048	0.102	0.203	0.847	54
Pseudomonadales	0.103	0.145	0.572	0.778	1548
Puniceispirillales	0.012	0.344	0.001	0.145	198
Rhodobacterales	0.000*	0.119	0.000*	0.016	576
Rhodospirillales	0.847	0.419	0.667	0.687	540
SAR11 clade	0.010	0.716	0.100	0.326	972
SAR324 clade (Marine group B)	0.012	0.619	0.115	0.699	72
Synechococcales	0.035	0.003	0.038	0.259	90
Photosynthetic microeukaryotes					
Bacillariophyta	0.275	0.487	0.004	0.122	576
Chlorellales	0.452	0.525	0.644	0.432	18
Chrysophyceae	0.000*	0.413	0.001	0.440	36
Cryptomonadales	0.001	0.041	0.001	0.043	NA
Dictyochophyceae	0.077	0.147	0.146	0.150	126
Euglenophyceae	0.625	0.366	N/A	N/A	126
Eustigmatophyceae	0.575	0.314	0.457	0.471	NA
Mamiellales	0.087	0.088	0.037	0.165	NA
Parmales	0.801	0.757	0.702	0.535	108
Pelagomonadales	0.864	0.636	0.641	0.874	54
Phaeocystales	0.140	0.024	0.446	0.320	18
Prymnesiales	0.495	0.145	0.281	0.440	180
Prymnesiophyceae	0.571	0.421	0.281	0.440	NA
Pyramimonadales	0.080	0.090	0.009	0.220	54
Ulvales relatives	0.179	0.413	0.221	0.424	36

* > 0.001

Table A8: Estimated effects of molecule type (DNA versus RNA) on relative abundance for dominant microbial orders
Reporting model term (molecule type), effect estimate, standard error, test statistic, degrees of freedom, and p value for each prokaryotic and photosynthetic microeukaryotic order.

Order	Term	Estimate	Std. Error	T statistic	df	p value
Prokaryotes						
Actinomarinales	Molecule type	-0.017	0.002	-11.136	24.699	0.000*
Burkholderiales	Molecule type	0.017	0.018	0.905	26.197	0.374
Cytophagales	Molecule type	0.001	0.001	0.676	26.120	0.505
Flavobacteriales	Molecule type	0.077	0.020	3.747	25.796	0.001
Marine Group II	Molecule type	-0.011	0.002	-5.008	24.381	0.000*
Marinimicrobia (SAR406 clade)	Molecule type	-0.006	0.001	-5.870	23.844	0.000*
Nitrosopumilales	Molecule type	-0.026	0.003	-7.999	27.509	0.000*
Parvibaculales	Molecule type	-0.008	0.001	-8.784	22.741	0.000*
Pseudomonadales	Molecule type	0.004	0.010	0.441	17.200	0.665
Puniceispirillales	Molecule type	0.007	0.002	3.994	25.796	0.000*
Rhodobacterales	Molecule type	0.015	0.006	2.669	26.022	0.013
Rhodospirillales	Molecule type	0.005	0.002	2.687	31.705	0.011
SAR11 clade	Molecule type	-0.166	0.011	-15.128	26.601	0.000*
SAR324 clade (Marine group B)	Molecule type	0.002	0.001	1.676	27.476	0.105
Synechococcales	Molecule type	0.088	0.009	9.671	26.048	0.000*
Photosynthetic microeukaryotes						
Bacillariophyta	Molecule type	0.338	0.030	11.164	26.365	0.000*
Chlorellales	Molecule type	-0.003	0.001	-3.911	26.898	0.001
Chrysophyceae	Molecule type	-0.013	0.013	-0.954	27.798	0.348
Cryptomonadales	Molecule type	-0.009	0.008	-1.136	26.046	0.266
Dictyochophyceae	Molecule type	0.000	0.002	-0.199	25.359	0.844
Euglenophyceae	Molecule type	0.000	0.000	-1.007	31.664	0.322
Eustigmatophyceae	Molecule type	0.000	0.000	-1.456	31.843	0.155
Mamiellales	Molecule type	-0.082	0.021	-3.981	25.213	0.001
Parmales	Molecule type	-0.011	0.003	-3.433	34.000	0.002
Pelagomonadales	Molecule type	0.000	0.000	-0.738	25.649	0.467
Phaeocystales	Molecule type	-0.219	0.032	-6.870	22.689	0.000*
Prymnesiales	Molecule type	0.000	0.000	0.190	34.000	0.851
Prymnesiophyceae	Molecule type	0.000	0.000	-1.000	34.000	0.324
Pyramimonadales	Molecule type	-0.002	0.001	-1.812	24.954	0.082

* > 0.001

Table A9: RDA axis contributions (%) from environmental variables for DNA and RNA for prokaryotes and photosynthetic microeukaryotes. Contributions of environmental variables to RDA1 and RDA2 axes (%) for DNA- and RNA-based community ordinations of prokaryotes and photosynthetic microeukaryotes, including DOM compound classes, carbon and nutrient concentrations, isotopic signatures, and salinity.

Environmental Variable	RDA1 (%) (DNA)	RDA2 (%)(DNA)	RDA1 (%) (RNA)	RDA2 (%) (RNA)
Prokaryotes				
Aliphatic	2.66	2.47	2.23	4.85
Aromatics	11.45	0.47	11.36	0.64
Condensed aromatics	10.42	0.57	11.06	0.84
DOC	0.96	0.87	0.97	1.98
DON	3.95	7.19	4.57	3.63
High-O Unsaturated	0.28	9.83	0.14	11.39
Low-O Unsaturated	0.26	2.12	0.28	3.62
NH_4^+	3.75	0.45	3.30	7.38
NO_3^-	10.25	1.07	10.12	0.46
PN	0.78	7.12	0.50	8.66
PO_4^{3-}	10.81	1.23	10.55	0.23
POC	0.36	38.27	1.38	41.13
Salinity	12.38	3.38	12.64	0.23
SiO_2	16.21	0.44	12.77	2.31
δ^{13}C-DOC	8.02	12.51	8.54	3.73
δ^{13}C-POC	4.35	6.27	5.45	6.25
δ^{15}N-PN	3.11	5.74	4.13	2.68
Photosynthetic microeukaryotes				
Aliphatic	2.99	0.27	1.89	10.03
Aromatics	11.74	0.28	10.72	10.22
Condensed aromatics	10.55	0.65	11.44	7.22
DOC	0.49	0.03	0.45	0.00
DON	3.44	3.76	4.12	0.01
High-O Unsaturated	0.28	6.99	0.06	13.00
Low-O Unsaturated	0.12	8.40	0.11	5.36
NH_4^+	3.16	1.35	1.72	5.36
NO_3^-	10.78	0.33	9.41	7.60
PN	0.63	0.02	0.86	0.40
PO_4^{3-}	11.19	0.52	9.60	7.20
POC	0.99	40.89	6.50	8.75
Salinity	12.12	1.13	11.18	6.12
SiO_2	14.26	1.47	8.17	14.33
δ^{13}C-DOC	8.72	2.11	9.69	3.37
δ^{13}C-POC	5.24	29.54	9.68	1.00
δ^{15}N-PN	3.29	2.26	4.41	0.02

Supplementary Methodology

Conservative Mixing

Conservative mixing plots measure the behaviour of DOC, POC, PN, and their respective isotopic signatures (δ^{13}C-DOC, δ^{13}C-POC, δ^{15}N-PN) across a salinity gradient between freshwater and marine end-members (Mori et al., 2019). The two end-members represent freshwater (0 PSU) and marine conditions (27.9 PSU, corresponding to the highest observed salinity). The fraction of freshwater (*f*) was calculated for each intermediate salinity value using Eq. A1 (St. Pierre et al., 2020), ranging from 1.00 at 0 PSU to 0.00 at 27.9 PSU. Expected conservative mixing values for each variable were computed at seven salinity intervals (0, 5, 10, 15, 20, 25, 27.9 PSU) based on the proportional contribution of each end-member (Eq. A2).

[Eq. A1] $f = \frac{S_{marine} - S_n}{S_{marine}}$
Where S_n is the salinity of the sample, and S_{marine} = 27.9 PSU.

[Eq. A2] $C_{expected} = f \times C_{freshwater} + (1 - f) \times C_{marine}$
Where $C_{freshwater}$ is the nutrient concentration/composition at a salinity of 0 PSU (freshwater), and C_{marine} is the nutrient concentration/composition at a salinity of 27.9 PSU (maximum salinity measured in Hyacinthe Bay).

Nutrient and Carbon Concentrations

All analytes were converted to micromolar (µM) units using molecular weights (12.01 g mol^{-1} C; 14.0067 g mol^{-1} N) (Eq. A3, A4). Replicate freshwater measurements (n=6) were averaged. Derived concentrations for TOC, DIN, DON (Eq. A5, A6, and A7), and stoichiometric ratios (e.g., POC:PN, TOC:TN, DOC:DON, N:P, DIN:TP) were calculated.

[Eq. A3] $Concentration\ in\ \mu M = \frac{Concentration\ in\ \mu\frac{g}{L}}{Molecular\ weight\left(\frac{g}{mol}\right)} \times 100$

[Eq. A4] $Concentration\ in\ \mu M = \frac{\frac{Volume\ of\ solvent\ (mL)}{POC\ measured\ (\mu g)}}{Molecular\ weight\left(\frac{g}{mol}\right)} \times 100$

[Eq. A5] $[TOC] = [POC] + [DOC]$

[Eq. A6] $[DIN] = [NH_4^+] + [(NO_3^- + NO_2^-)]$

[Eq. A7] $[DON] = [TDN] - [DIN]$

Biological Limiting Nutrient

Nutrient limitation was inferred from the molar ratio of dissolved inorganic nitrogen (DIN) to total phosphorus (TP), where values <16 indicate nitrogen limitation and >16 indicate phosphorus limitation (Ptacnik et al., 2010) (Eq. A8).

[Eq. A8] $DIN{:}TP = \frac{DIN}{TP}$

Fourier Transform Ion Cyclotron Resonance Mass Spectrometry (FT-ICR-MS)

Molecular formulae and bulk metrics were derived from ultrahigh-resolution FT-ICR-MS data according to established protocols (Koch & Dittmar, 2006; Qi et al., 2022; Ren et al., 2024) (Eq. A9).

[Eq. A9] $AI_{mod} = \frac{1+C-0.5H-0.5X}{C-0.5X}$
$where\ C, H = number\ of\ carbon\ and\ hydrogen\ atoms\ and\ X = number\ of\ O, N, S, and\ P\ atoms\ (heteroatoms)$

Microbial Community Composition Analysis

[Eq. A10] $Relative\ abundance = \frac{Count}{sum(Count)}$

[Eq. A11] $DNA{:}\,RNA = \frac{RNA\ relative\ abundance}{DNA\ relative\ abundance}$